2021

Virus-Like Particles Enable Low Levels of CRISPR-Cas9-Mediated Homology-Directed Repair

Noah C. Cheng , '21

Virus-Like Particles Enable Low Levels of CRISPR-Cas9-Mediated Homology-Directed

Repair

Noah Cheng

Department of Biology, Swarthmore College

Jennifer Hamilton, University of California, Berkeley, Thesis Mentor

Amy Vollmer, Swarthmore College, Faculty Liaison

ABSTRACT

The development of efficient and safe delivery platforms for CRISPR-Cas9 genome editing tools is one of the largest challenges for *in vivo* therapeutic genome editing. Virus-like particles (VLPs), which harness viral packaging and delivery mechanisms, have been shown to efficiently deliver CRISPR-Cas9 ribonucleoprotein complexes (RNPs) to cells. Here, we sought to elucidate whether VLPs can deliver the necessary components for CRISPR-Cas9-mediated homology-directed repair (HDR). We tested four different methods to induce HDR in a reporter cell line using VLPs: [1] nucleofection of HDR repair templates into cells and subsequent treatment with VLPs carrying Cas9 RNPs (Cas9 VLPs), [2] treatment with Cas9 VLPs loaded with repair templates through electroporation, [3] treatment with VLPs packaging both Cas9 RNPs and a lentiviral genome that encoded the repair template, and [4] treatment with Cas9 VLPs and VLPs carrying just the HDR template encoded on the lentiviral genome (dual-VLP system). We found that VLPs enabled CRISPR-Cas9-mediated HDR, albeit at low frequencies. HDR efficiency was highest when the HDR template was nucleofected into the cells, but appreciable levels of HDR was also observed using the dual-VLP system. This work suggests that VLPs are a viable delivery platform for the necessary components for CRISPR-Cas9-mediated HDR, but considerable improvements in the platform must be made before it is used in therapeutic settings.

INTRODUCTION

Therapeutic genome editing has the enormous promise to treat and possibly cure human genetic-based diseases. To actualize this potential, effective and safe genome editing tools must be developed. In general, genome editing tools target and modify specific DNA sequences, potentially leading to changes in an organism's phenotype (*1*, *2*). Clustered regularly interspaced short palindromic repeats (CRISPR)-based tools are now the most commonly used genome editing technologies, but other genome editing tools exist, such as zinc-finger nucleases (ZFNs) and transcription activator-like effector nucleases (TALENs).

Genome Editing Strategies and Methods

ZFNs are composed of concatenated zinc finger domains, which are common DNA-binding motifs, fused to the nonspecific DNA cleavage domain of the *FolkI* restriction

2

enzyme (*3*). Each zinc finger domain recognizes 3-4 base pairs of DNA, and thus an array of

zinc finger domains can recognize specific sequences of contiguous DNA (*2*, *3*). To induce a

double stranded break (DSB), two ZFNs must bind on opposite strands of DNA such that the

FolkI domain on each ZFN cuts the DNA within a specified spacer sequence (*3*). Discovered in

the bacteria genus *Xanthomonas*, transcription activator-like effector (TALE) proteins have

DNA-binding domains that are composed of highly conserved amino acid repeats in tandem (*2*,

4). Each TALE repeat binds to a specific nucleotide, so multiple TALE repeats can be artificially

linked together to produce an array of TALEs that recognizes a specific DNA sequence (*2*, *4*).

Similar to ZFNs, TALENs are generated by fusing the nonspecific *FokI* cleavage domain to an

array of TALE repeats, and two TALEN monomers are needed to create a DSB (*2*, *4*).

　　Both ZFNs and TALENs have shown promise for use in therapeutic genome editing. For

example, ZFNs have been used to knock out the gene encoding the human immunodeficiency

virus (HIV) co-receptor, CCR5, in human hematopoietic stem cells. Highly immunodeficient

mice engrafted with these ZFN-edited cells were able to control HIV replication (*5*).

Additionally, primary human T cells have been edited with TALENs and then transduced with a

chimeric antigen receptor (CAR) to produce CAR-T cells that have the *TRAC* and *CD52* genes

disrupted (*6*). Disrupting *TRAC*, which encodes the endogenous T cell receptor, produces CAR-T

cells that can be used in any individual, as no alloreactive TCR will be present and thus

graft-versus-host disease will be avoided. Disrupting *CD52* yields cells that can persist in the

presence of a chemotherapeutic agent, alemtuzumab, which typically targets CD52 and depletes

lymphocytes (*6*). While ZFNs and TALENs can mediate therapeutic genome editing, they remain

relatively laborious to design and produce.

Easily programmed and highly efficient, CRISPR technology has revolutionized the field of therapeutic genome editing. CRISPR/CRISPR-associated (Cas) systems were originally identified as a form of adaptive immunity in bacteria, allowing microorganisms to record bacteriophage infections and then mount a faster defense response upon reinfection (*7*). CRISPR-Cas systems contain *cas* genes and CRISPR arrays, which are composed of alternating spacer sequences and 20-50 bp identical repeats (*7, 8*). The spacer sequences are complementary to specific sequences of DNA (protospacers), such as a portion of a bacteriophage genome. Transcription of spacer repeats and cleavage of the subsequent transcripts produce CRISPR RNA (crRNA) molecules (*7, 8*). In type II CRISPR-Cas systems, crRNA complexes with trans-activating crRNA (tracrRNA) and then guides the Cas9 protein to the protospacer sequence where Cas9 induces a DSB (*8*). Cas9-mediated cleavage also requires a protospacer adjacent motif (PAM) that is adjacent to the target sequence (*8*). To harness the CRISPR-Cas system for genome editing, chimeric single guide RNAs (sgRNAs), which combine the essential components of crRNAs and tracrRNAs, can be easily designed and produced to target specific genomic sequences for Cas9-induced cleavage (*8*).

A Cas9-generated DSB is then repaired through one of several endogenous repair pathways. Most commonly, the cleavage is repaired through non-homologous end joining (NHEJ), which creates random insertions or deletions (indels). Alternatively, homology-directed repair (HDR), which is less favored in human cells compared to NHEJ, uses a repair template to resolve the cleaved DNA (*9*). The repair template can be a sister chromatid or an exogenous piece of DNA. In HDR, the production of a DSB is followed by 5' -> 3' DNA resection (*9*). The resection reveals homologies between the repair template and the sequence surrounding the DSB (*9*). Depending on whether the repair template is single- or double-stranded, different pathways

are activated to repair the break using the template (*9*). In relation to genome editing, NHEJ typically generates gene knockouts, while HDR can produce gene knock-ins, mediate deletions, and direct any base conversion. In principle, by designing specific repair templates, one can harness HDR to completely correct human genetic-based disorders. Thus, many studies have attempted to increase the efficiency of Cas9-mediated HDR in mammalian cells. For instance, it has been demonstrated that HDR efficiency can be increased by inhibiting key molecules in the NHEJ repair pathway (*10*). However, inhibiting molecules in the NHEJ pathway may impair the cell's capacity to fix DNA damage at other sites and thus may not be optimal for therapeutic genome editing (*11*). Alternatively, Richardson and colleagues increased HDR frequencies using a single-stranded, asymmetric donor template that was designed based on how the Cas9 protein interacts with its DNA substrate (*11*).

Delivery Methods

In addition to increasing the frequency of HDR, another large challenge in therapeutic genome editing is the development of strategies to safely and efficiently deliver genome editing tools and any repair templates into cells. *Ex vivo* delivery of CRISPR-Cas9 technology can be achieved through electroporation of preformed Cas9-sgRNA ribonucleoprotein complexes (RNPs) (*1*). For example, autologous hematopoietic stem cells have been electroporated with Cas9 RNPs that target the enhancer region of the *BCL11A* gene, which encodes a protein that represses γ-globin expression. Cas9 editing results in reduced expression of *BCL11A*, subsequently leading to reactivation of γ-globin expression and to increased synthesis of fetal hemoglobin. Preliminary reports suggest that transplantation of these edited cells into the bone marrow can successfully treat patients with sickle cell disease (*12*). While *ex vivo* genome

editing can be applied immediately to hematopoietic stem cell and immune cell therapies, for example, *in vivo* genome editing has perhaps more promise, as it circumvents the need for bone marrow transplantation (*1*, *13*). However, *in vivo* delivery of genome editing tools remains considerably more challenging than *ex vivo* delivery. The optimal *in vivo* delivery platform must confer tissue specificity, prevent genomic integration, limit off-target effects, induce low immunogenicity, and show relatively high efficiency. The ideal delivery vehicle for *in vivo* applications would further control the duration of genome editing activity, as prolonged activity could increase the number of off-target events and induce immune reactions (*1*).

Viral delivery mechanisms, such as adeno-associated viruses (AAVs), offer many advantages. In fact, AAVs are commonly used in gene therapy clinical trials, suggesting that this delivery vehicle can also be utilized for therapeutic genome editing (*13*). AAVs have relatively low immunogenicity, and in the cell, the viral genome either exists as an episome or integrates at the neutral human AAVS1 locus (*1*, *13*). Additionally, AAVs have a broad range of serotypes with tropism for different tissues (*13*). Given its many advantages, the AAV delivery platform has been used frequently for *in vivo* genome editing. For example, AAVs carrying CRISPR-Cas9 technology have been used to treat Duchenne muscular dystrophy and Leber congenital amaurosis type 10 (LCA10) in mice (*14*, *15*). In fact, a current human clinical trial is using an AAV vector to deliver the CRISPR technology necessary for treatment of LCA10. This trial marks the first instance of *in vivo* human genome editing with CRISPR-Cas9 (*16*). Furthermore, Yang and colleagues developed a dual AAV system that delivered the necessary CRISPR-Cas9 components to newborn mice to correct a mutation that causes metabolic liver disease (*17*). Specifically, one AAV vector carried the Cas9 protein while the other vector encoded the guide RNA and a donor HDR template (*17*). Nonetheless, there are still disadvantages to using AAVs

for the therapeutic delivery of genome editing tools. For instance, long-term expression of the CRISPR-Cas components can lead to off-target editing and/or increased immunogenicity (*1*). Moreover, the AAV genome can harbor roughly 4.7 kilobases (kb) of genetic information, but the most commonly used *Streptococcus pyogenes* Cas9 (SpCas9) protein is encoded by a 4.2 kb gene (*1*, *13*). This challenge can be addressed by delivering the Cas9 protein and the sgRNA in separate AAV vectors and/or by using the *Staphylococcus aureus* Cas9 protein, which is encoded by a ~3.2 kb gene and thus much smaller than SpCas9 (*14*, *15*, *17–19*). Using multiple AAV vectors, however, may reduce editing efficiency, because editing activity relies upon cellular co-infection.

Lipid nanoparticles (LNPs) are alternate delivery vehicles that have several advantages over AAV vectors. Unlike AAVs, LNPs can carry either mRNA encoding Cas9 or pre-formed Cas9 RNPs. They are easily produced by mixing mRNA or Cas9 RNPs, both of which have anionic properties, with cationic lipid nanoparticles (*20–22*). By delivering CRISPR-Cas9 technology in the form of mRNA or RNPs, LNPs facilitate transient gene editing and avoid any genomic integration (*1*). Moreover, while the size of AAVs is roughly 20 nm, the size of LNPs is adjustable and ranges between 50 nm and 500 nm (*13*). Several studies have shown efficient *in vivo* genome editing in the mouse liver using an LNP delivery system (*21*, *22*). For example, LNPs have been used in combination with AAVs to enable Cas9-mediated treatment of hereditary tyrosinemia in mice (*22*). In this study, the LNPs delivered Cas9 mRNA while the AAVs encoded a sgRNA expression cassette and an HDR template (*22*). Despite their advantages over other delivery platforms, LNPs currently lack the ability to target specific tissues other than the liver tissue when delivered systemically, limiting their potential to be a widely and clinically applicable delivery strategy for non-hepatic cellular targets (*1*).

Like AAVs, lentiviral vectors are frequently used in gene therapy trials and provide tissue specificity (*13*, *23*). However, random genomic integration can occur after reverse transcription of the lentiviral RNA genome, and if this integration occurs close to a proto-oncogene, malignant transformations may ensue (*13*, *23*). Thus, lentiviral vectors are not a feasible delivery mechanism for CRISPR system components. As an alternative to lentiviral vectors, lentivirus-like particles (VLPs) lack the capacity to replicate and integrate viral genomic information but retain the structural and envelope proteins that facilitate fusion with certain cells. Pseudotyped VLPs that target specific tissues and cells can be produced by co-expressing the lentiviral structural Gag polyprotein with a viral envelope protein in cultured cells (*23*, *24*) (Fig. 1a). Additionally, it has been shown that proteins, such as Cas9, can be fused to the Gag polyprotein and then encapsulated in pseudotyped VLPs (*23*, *24*) (Fig. 1b). Thus, similar to LNPs, VLPs can package and deliver pre-formed Cas9 RNPs, leading to transient genome editing (*24*). The size of VLPs carrying Cas9 RNPs has been estimated to be 150 nm (*24*). Like all other delivery strategies, VLPs also have disadvantages. Immune reactions against VLPs are certainly possible, and the virions can only package a limited number of RNPs. Nonetheless, VLPs are, in theory, an optimal delivery platform for CRISPR technology, as they allow for tissue targeting, prevent genomic integration, avoid long-term expression of the Cas9 protein, and promote relatively high editing efficiencies (*24*). Moreover, while it has not been thoroughly investigated, it is likely that VLP-mediated off-target effects would be reduced compared to stable delivery methods (*24*). VLPs deliver RNPs, and off-target editing is relatively infrequent when using RNPs (*25*, *26*).

While VLPs have been shown to enable both *in vitro* and *in vivo* Cas9-mediated editing (*24*), the capacity of VLPs to also direct gene repair via HDR has not been widely studied. Mangeot and colleagues demonstrated that Cas9 RNP-carrying VLPs complexed with a donor

DNA template ("All-in-one" Nanoblades) could induce HDR (*24*). To produce these "All-in-one" Nanoblades, they combined VLPs and a DNA template in a solution containing polybrene (*24*), which has been shown to increase the efficiency of viral glycoprotein-mediated DNA transfection (*27*). As a result, the template was associated with the outside of the virion. However, this group did not test ways to incorporate HDR templates into the VLPs, and the HDR efficiency in a population of transduced cells was either not rigorously quantified or extremely low (roughly 42 edited cells in a population of 1 x 10^5 transduced cells) (*24*). Thus, more research must be undertaken to determine whether VLPs are capable of efficiently delivering the necessary components for Cas9-mediated HDR.

Our Studies

Here, we tested several methods to deliver HDR repair templates and Cas9 RNPs using VLPs and thus investigated whether VLPs could direct gene repair via HDR.

[1]To begin, we confirmed that VLPs carrying Cas9 RNPs could enable HDR when the donor template was nucleofected into cells. Others have shown that nucleofection is an efficient delivery mechanism for HDR templates (*11*).

[2] Yamada and colleagues demonstrated that hepatitis B virus-like particles produced in yeast cells could be electroporated with green fluorescent protein (GFP) expression plasmids and subsequently used to deliver the plasmids to cells (*28*). We therefore reasoned that VLPs carrying Cas9 RNPs could be electroporated with HDR templates, generating VLPs that could deliver all the necessary components for Cas9-mediated HDR in one step.

[3] Integrase-defective VLPs with a lentiviral genome can also be designed. In these VLPs, the lentiviral genome is not integrated and instead forms an episome. Thus, we produced VLPs that contained both Cas9 RNPs and a lentiviral genome that encoded the HDR template.

[4] Preliminary results suggested that co-packaging Cas9 RNPs and a lentiviral genome into VLPs impaired transduction efficiency, so we tested a dual-VLP strategy in which the Cas9 RNPs and the lentiviral genome encoding the HDR template were delivered in separate VLPs.

If VLPs were able to efficiently deliver all the components necessary for Cas9-mediated HDR, we would have expected to record HDR frequencies similar to those found when the Cas9 RNP and template are both nucleofected into cells (~10-50%) (*11*).

MATERIALS and METHODS

Cell Lines

A blue fluorescent protein (BFP) human embryonic kidney (HEK) 293T reporter cell line (hereafter called BFP 293T) allows for the identification and quantification of unedited, NHEJ, and HDR populations following CRISPR-Cas9 editing (Fig. 2). In this cell line, a 196C -> T substitution results in the conversion of the *BFP* gene to the *GFP* gene *(11, 29)*. Following Cas9-mediated cleavage in the *BFP* gene, the cell can undergo NHEJ, which results in indel formation and loss of *BFP* expression. If a donor DNA template encoding the single-base pair substitution is provided, HDR can occur, after which the cell would express *GFP*. Lenti-X HEK 293T cells (Takara Bio) were used to produce VLPs. Lenti-X and BFP 293T cells were cultured in DMEM that contained 10% Fetal Bovine Serum and 100 units/mL Penicillin-Streptomycin (cDMEM).

<u>Plasmids and HDR Templates</u>

Eight different plasmids were used in this study (Table 1). Transcription of the Gag-Pol plasmid and subsequent, natural frameshifting during translation results in the production of both the Gag and Gag-Pol polyproteins, although the frequency of Gag-Pol expression is roughly 5% of the frequency of Gag expression (*30*). Transfection of cells with the VSV-G and Gag-Pol plasmids is sufficient to produce glycoprotein-containing VLPs (Fig. 1a). The sgRNA and transfer genome plasmids were constructed through cloning. First, we cloned a *BFP*-targeting sgRNA into a U6 expression plasmid, such that the sgRNA sequence was under control of the U6 promoter. Second, a double-stranded version of the HDR template was cloned into a vector encoding an HIV-1 transfer genome (Table 1). Lastly, Golden Gate Cloning was used to concatenate multiple copies of the HDR template on the HIV-1 transfer genome.

The HDR template used in this study directed a three base-pair conversion in the *BFP* gene. These mutations, including the 196C -> T substitution, changed the gene to *GFP* and concomitantly destroyed the PAM sequence such that the Cas9 protein could not cleave the DNA again. Three different variations of the HDR template were tested: [1] the <u>target strand HDR donor</u> was a ssDNA template largely identical to the strand of DNA targeted by the sgRNA; [2] the <u>nontarget strand HDR donor</u> was a ssDNA template complementary to the strand of DNA targeted by the sgRNA; [3] the <u>annealed HDR donor</u> was a dsDNA template formed by annealing the two ssDNA templates. Unless otherwise specified, the HDR template used in the experiments was the target strand HDR donor, as others have found that target strand HDR repair templates are most effective (*11*).

VLP Production and Collection

Lenti-X cells were plated at 3.7 x 10^6 cells/ml in cDMEM and placed in an incubator at 37°C and 5% CO_2. On the following day, polyethylenimine was used to transfect Lenti-X cells with 1 µg, 3.3 µg, 6.7 µg, and 10 µg of the VSV-G, Gag-Pol (psPax2), Gag-Cas9, and sgRNA plasmids, respectively (Fig. 1b). The sgRNA plasmid encoded a sgRNA that targeted either the *B2M* or *BFP* gene. Unless otherwise specified, the Cas9 RNPs packaged into VLPs targeted the *BFP* gene. To produce VLPs containing Cas9 RNPs and a lentiviral genome, Lenti-X cells were also transfected with 10 µg of the transfer genome plasmid, and the integrase- defective psPax2-D64V was used instead of psPax2 (Fig. 5b). When generating VLPs that carried the lentiviral genome alone, cells were transfected with 1 µg, 10 µg, and 10 µg of the VSV-G, psPax2-D64V, and transfer genome plasmids, respectively.

The VLP-containing supernatant was collected 48 hours post-transfection, spun at 1000 RPM at room temperature for 5 minutes, and then filtered through a 0.45 µm filter. VLPs were concentrated via ultracentrifugation. In an ultracentrifuge tube, the filtered supernatant was placed on top of 3 mL of 30% (w/v) sucrose in NTE (100 mM NaCl, 10 mM Tris-HCl pH 7.5, 1 mM EDTA pH 8.0) and then ultracentrifuged at 25k and 4°C for 1 hour and 45 minutes. Following ultracentrifugation, the liquid was removed from the tubes and the VLPs were resuspended in Opti-MEM. VLPs were considered 1X concentrated when the VLPs collected from one 100 mm plate of Lenti-X cells were eventually resuspended in 1 mL of Opti-MEM.

Nucleofection Experiments

A Lonza 4D-Nucleofector and Lonza 4D Nucleocuvette Strip were used for nucleofection. In each compartment of the Nucleocuvette, 2x10^5 BFP 293T cells resuspended in

20 µL of SF solution (82% SF Cell Line Nucleofector Solution + 18% Supplement 1) were mixed with 100 pmol of HDR template or 1 µg of a GFP-expressing plasmid. The cells were nucleofected in the Lonza 4D-Nucleofector using the DS150 setting. Following nucleofection, each mixture was supplemented with 100 µl cDMEM and then incubated at room temperature for 10 minutes. After the incubation period, each nucleofected cell solution was transferred to one well in a 24-well culture plate. In the first experiment, 1 mL of 0.6X concentrated VLPs carrying anti-*BFP* Cas9 RNPs ("Cas9 VLPs") was added to each well after the cells had been plated (final volume was ~1.12 mL). In the second experiment, prior to adding the nucleofected cells, 600 µL of 10X concentrated VLPs and 400 µL of Opti-MEM were combined in a well. Serial 2-fold dilutions in Opti-MEM were made across the plate, and then the nucleofected cells were plated for expansion and subsequent analysis (final volume in each well was ~620 µL).

For both experiments, to determine HDR frequency when a DSB was not induced, we performed a control in which BFP 293T cells were nucleofected with the HDR template but were not treated with VLPs. A corresponding amount of Opti-MEM was added instead of the VLP solution. Additional controls were performed in the first nucleofection experiment. In the VLP-only control, cells were nucleofected without the HDR template and then treated with VLPs, effectively confirming that HDR will not occur if a donor template is not present. Moreover, a positive control ("GFP Plasmid") was conducted to validate the efficacy of the nucleofection protocol. For this control, BFP 293T cells were nucleofected with a GFP plasmid but were not treated with VLPs. Lastly, in the Cells Only control, cells were neither nucleofected nor treated with VLPs.

<u>Electroporation Experiments</u>

A sample containing 500 µL of 0.95X concentrated anti-*B2M* or 0.78X concentrated anti-*BFP* Cas9 VLPs in Opti-MEM was added to a 4 mm gap electroporation cuvette and kept on ice until electroporation. Then, 100 pmol of HDR template or 1 µg of mNeonGreen plasmid was added to the cuvette. The mixtures were electroporated in a Gene Pulser Xcell for ~20 ms at 220 V and 950 µF. When electroporating the mNeonGreen plasmid into anti-*B2M* VLPs, different resistance settings were tested. Our results indicated that 200 ohms was the most effective resistance, so for all other electroporation experiments, the resistance was set at 200 ohms. Following electroporation, the solutions were immediately placed back on ice.

To test these electroporated VLPs, 200 µL of an electroporated mixture was added to each well in the first column of a 96-well culture plate, and 100 µL of Opti-MEM was placed in the rest of the wells. Serial 2-fold dilutions were carried out across the plate, and then 1.5×10^4 BFP 293T cells were added to each well (final volume was 150 µL). We also performed negative controls in which cells were not treated with VLPs.

<u>Experiments with VLPs Packaging Cas9 RNPs and a Lentiviral Genome</u>

VLPs that co-packaged anti-*BFP* Cas9 RNPs and a lentiviral genome encoding 0 to 3 copies of the HDR template were produced ("Super VLPs"). To determine the efficacy of Super VLPs, 100 µL of the appropriate 5X concentrated Super VLPs and 1.5×10^4 BFP 293T cells were combined (final volume was 150 µL). We wanted to determine whether BFP knockout frequency was affected after adding the lentiviral genome to Cas9 VLPs, so we performed a control that treated cells with the same volume of 5X concentrated Cas9 VLPs. Lastly, an untreated, Cells Only control was also carried out.

<u>Experiments Using Two VLPs (Dual-VLP System)</u>

Anti-*BFP* Cas9 VLPs and VLPs with a lentiviral genome encoding 0 to 3 copies of the HDR template were produced ("HDR VLPs"). In our first experiment, we treated BFP 293T cells with the two different VLPs at different time points. Specifically, 1.5×10^4 BFP 293T cells were transduced with 100 µL of 1X concentrated HDR VLPs carrying one template within the lentiviral genome. Roughly 24 hours later, 100 µL of 1X concentrated Cas9 VLPs was added (final volume was 250 µL). Next, we treated 1.5×10^4 BFP 293T cells simultaneously with 100 µL of 1X concentrated HDR VLPs carrying one template and 100 µL of 1X, 2X, or 8X concentrated Cas9 VLPs (final volume was 250 µL). A similar experiment was performed in which 1.5×10^4 BFP 293T cells were treated simultaneously with 100 µL of 1X concentrated Cas9 VLPs and 100 µL of 1X, 2X, or 10X concentrated HDR VLPs carrying one template (final volume was 250 µL). In the last experiment, BFP 293T cells were treated with Cas9 VLPs and HDR VLPs encoding 0, 1, 2, or 3 HDR templates in the lentiviral genome. Specifically, 1.5×10^4 cells were transduced with 50 µL of 2X concentrated Cas9 VLPs and 50 µL of 2X concentrated HDR VLPs carrying a certain number of HDR templates (final volume was 150 µL).

In all of these experiments, controls were performed to observe BFP knockout and HDR frequencies when one of the two VLPs was omitted. In these controls, a corresponding amount of Opti-MEM was used instead of the Cas9 or HDR VLPs. Two of the experiments included Cell Only controls that revealed editing frequencies when no VLPs were added.

<u>Flow Cytometry and Data Analysis</u>

Cells were resuspended in phosphate-buffered saline for flow cytometry on days 3 and 7 post-transduction. An Attune Nxt flow cytometer (ThermoFisher Scientific) was used to quantify

editing frequencies (percentage of cells in transduced population with a given editing outcome). In each transduced cell population, both BFP knockout and HDR frequency was measured. For the nucleofection and electroporation experiments, we used GFP fluorescence as a measurement of HDR frequency. HDR frequency was not quantified by measuring the percentage of BFP-/GFP+ cells, because cells that underwent HDR could still have residual BFP protein that had not turned over. For the experiments in which the template was delivered via the lentiviral genome, we quantified HDR frequency by recording the percentage of mCherry and GFP double-positive cells (Fig. 5d).

Statistical Analysis

In the experiments testing the dual-VLP system, an ANOVA was performed to determine whether the concentration of one or both of the VLPs affected BFP knockout and HDR frequencies. Given the small sample size of n=3, normality tests would have limited statistical power and thus were not performed. While ANOVAs are insensitive to violations of normality (*31*, *32*), they are sensitive to the lack of homogeneity of variance. However, it has been shown that *F*-test is robust when sample sizes are equal across treatments (*33*). We therefore reasoned that an ANOVA was appropriate. If the ANOVA revealed significance, Tukey's post hoc test was then used for pairwise comparisons of editing frequencies between treatments. An ANOVA was also used to compare mCherry+ and HDR frequencies in cells transduced with Cas9 VLPs and HDR VLPs carrying 0 to 3 copies of the repair template on the lentiviral genome. If appropriate, pairwise comparisons were performed using Tukey's post hoc test. Statistical analyses were performed in R Studio, and the significance level in all tests was 0.05.

RESULTS

<u>High HDR frequencies were observed when cells were nucleofected with HDR templates and subsequently treated with Cas9 VLPs</u>

We wanted to confirm that Cas9 VLPs could enable HDR when the donor DNA template was nucleofected into cells (Fig. 3a). The high GFP fluorescence signal in cells nucleofected with the GFP control plasmid confirmed that the nucleofection protocol was efficient (Fig. 3b). Disruption of *BFP* expression was not yet measurable 3 days after VLP treatment, as the majority of the BFP protein had not turned over yet (Fig. 3b left panel). By day 7 post-transduction, BFP knockout frequency had reached above 80% in cells treated with 1 mL of 0.6X concentrated Cas9 VLPs. BFP knockout was largely undetectable in the controls that were not treated with Cas9 VLPs. Relatively high levels of HDR (~24%) were achieved when cells were nucleofected with the HDR template and transduced with 1 mL of 0.6X concentrated Cas9 VLPs (Fig. 3b right panel). Some cell populations became contaminated, so certain trials and conditions were not passed following flow cytometry analysis on day 3.

In attempts to increase HDR efficiencies, we recorded editing outcomes when nucleofected cells were treated with higher concentrations of Cas9 VLPs. Most noticeably, VLPs enabled CRISPR-Cas9 genome editing in a dose-dependent manner. When nucleofected cells were treated with 500 µL of 1.5X or greater concentrated VLPs, close to 100% of cells showed BFP knockout and roughly 35% of cells underwent HDR (Fig. 3c). Three distinct populations of cells (WT, NHEJ, and HDR) could be distinguished by flow cytometry analysis. The HDR and NHEJ cell populations were largely absent when cells nucleofected with the HDR template were not treated with VLPs (Fig.3d).

<u>Cas9 VLPs loaded with HDR templates via electroporation facilitated low levels of HDR</u>

As a proof-of-concept and to optimize electroporation conditions, we determined whether anti-*B2M* Cas9 VLPs electroporated with a mNeonGreen-expressing plasmid could deliver the plasmid to cells. When BFP 293T cells were transduced with 100 µL of 0.95X concentrated VLPs electroporated at 200 ohms, 0.39% ± 0.18% of cells were mNeonGreen+. VLPs electroporated at other resistances were not as efficient at delivering the mNeonGreen plasmid to cells. Almost no fluorescence was detected in cells treated with VLPs that were in solution with the mNeonGreen plasmid but were not electroporated (Fig. 4b).

After demonstrating that VLPs could be electroporated to carry exogenous pieces of DNA, we sought to investigate whether HDR templates could be packaged into the anti-*BFP* Cas9 VLPs through electroporation (Fig. 4a). Electroporated Cas9 VLPs directed BFP knockout in a dose-dependent manner. The kind of template electroporated into the VLP did not appear to affect BFP knockout frequency (Fig. 4c top panel). At the highest relative concentration tested, Cas9 VLPs electroporated with the target strand donor enabled higher frequencies of HDR (0.32% ± 0.31%) than those electroporated with the nontarget strand donor (0% ± 0%) and the annealed donor (0.029% ± 0.040%). Interestingly, cells treated with VLPs that were in solution with the target strand donor but were not electroporated showed detectable levels of HDR (0.23% ± 0.078%) (Fig. 4c bottom panel).

<u>Super VLPs did not enable high frequencies of HDR</u>

We reasoned that integrase-defective Cas9 VLPs could also be packaged with an HIV-1 transfer genome encoding the HDR template (Fig. 5a). Similar to VLPs electroporated with the template, these Super VLPs had all the necessary components for Cas9-mediated HDR enclosed

in one VLP. BFP knockout frequency in cells treated with 100 µL of 5X concentrated VLPs

decreased considerably when the lentiviral genome was packaged into Cas9 VLPs. Knockout

frequency continued to decrease dramatically as more HDR templates were added to the

lentiviral genome. In fact, disruption of *BFP* expression was rarely detected in cells transduced

with Super VLPs encoding 2 or 3 copies of the template (Fig. 5c left panel). Only cells treated

with Super VLPs encoding 1 copy of the HDR template showed detectable levels of HDR (Fig.

5c right panel).

Appreciable levels of HDR were achieved when Cas9 and HDR VLPs were used in combination

Given the ineffectiveness of Super VLPs, we sought to determine whether HDR can be

enabled by a dual-VLP system in which Cas9 RNPs and the HIV-1 transfer genome encoding the

HDR template were packaged into separate VLPs (Fig. 6a). When cells were first treated with

100 µL of 1X concentrated HDR VLPs and then treated 1 day later with 100 µL of 1X

concentrated Cas9 VLPs, appreciable levels of HDR were detected (0.35-0.74%) (Fig. 6b right

panel). In this experiment, BFP knockout frequencies were similar in the Cas9 VLP + HDR VLP

and the Cas9 VLP Only treatments (Fig. 6b left panel). Interestingly, HDR VLPs alone also

appeared to facilitate low levels of HDR in the 293T cells (Fig. 6b right panel). These results

indicated that this dual-VLP system was relatively effective.

Thus, we reasoned that increasing the concentration of one of the VLPs might increase

HDR frequency. In the following two experiments, 100 µL of each VLP was used to treat cells.

As expected, Cas9 VLP concentration impacted the BFP knockout frequency in cells treated

simultaneously with Cas9 and HDR VLPs ($F_{2,6}$=202, p<0.001). BFP knockout levels increased

significantly as the concentration of Cas9 VLPs increased (p<0.01) (Fig. 6c left panel). In the

dual-VLP system, Cas9 VLP concentration did not significantly impact HDR frequency ($F_{2,6}$=0.6996, p=0.533). Cells transduced with 1X concentrated HDR VLPs and 1X, 2X, or 8X concentrated Cas9 VLPs exhibited median HDR levels of 0.78%, 0.66%, and 0.59%, respectively (Fig. 6c right panel). We next kept the concentration of Cas9 VLPs constant and increased the concentration of HDR VLPs. Unexpectedly, in the dual-VLP system, HDR VLP concentration had a significant effect on BFP knockout frequency ($F_{2,6}$=6.427, p=0.0322). Cells treated with 1X concentrated Cas9 VLPs and 10X concentrated HDR VLPs showed greater HDR levels than those treated with 1X concentrated Cas9 and HDR VLPs (p=0.0349) (Fig. 6d left panel). However, this finding could simply be a result of our small sample size. Levels of HDR fluctuated when cells were treated with Cas9 VLPs and increasing concentrations of HDR VLPs ($F_{2,6}$=9.385, p=0.0142). Cells transduced simultaneously with 1X concentrated Cas9 VLPs and 10X concentrated HDR VLPs showed the highest median HDR frequency (0.59%) (Fig. 6d right panel). In fact, these cells had significantly higher HDR levels than those treated simultaneously with 1X and 2X concentrated Cas9 and HDR VLPs, respectively (p=0.0122). In both of these experiments, appreciable levels of HDR were measured when cells were treated with HDR VLPs alone (Fig. 6c,d). No HDR was detected when cells were not treated with HDR VLPs (Fig. 6c,d).

Lastly, we tested the dual-VLP system when the HDR VLPs carried more than one copy of the HDR template in their genome. Cells simultaneously transduced with 50µL of 2X concentrated Cas9 VLPs and 50 µL of 2X concentrated HDR VLPs encoding 0, 1, 2, or 3 templates had minimal amounts of HDR 3 days post-transduction. Treatment with Cas9 VLPs and HDR VLPs encoding 1 copy of the HDR template led to very low levels of HDR (median 0.034%) (Fig. 6e). The number of repair templates carried by the HDR VLPs did not affect the HDR frequency in cells treated using the dual-VLP system ($F_{3,8}$=1.073, p=0.4133).

<u>Transduction efficiency of Super and HDR VLPs decreased as the number of HDR templates encoded on the lentiviral transfer genome increased</u>

Interestingly, we observed that VLPs encoding 2 or 3 copies of the HDR template on the lentiviral genome were ineffective at enabling HDR. In attempts to understand the reasoning behind this observation, we analyzed the transduction efficiencies of VLPs carrying a lentiviral genome. For both Super and HDR VLPs, transduction efficiency, as measured by mCherry+ frequency in treated cells, decreased as more templates were added to the HIV-1 transfer genome (Table 2). A statistical analysis was used to compare transduction efficiency between HDR VLPs carrying different numbers of HDR templates in the dual-VLP system ($F_{3,8}$=1577, p<0.001). HDR VLP transduction efficiency decreased significantly for each added repair template on the lentiviral genome (p<0.05) (Table 2). Furthermore, comparing the transduction efficiencies of Super and HDR VLPs, HDR VLPs appeared to be more effective at delivering each version of the lentiviral genome, even though they were tested at a lower concentration than the Super VLPs (Table 2). Lastly, HDR VLPs transduced more cells when used alone than when used in combination with Cas9 VLPs (Table 2).

DISCUSSION

The ability to deliver genome editing tools safely and efficiently *in vivo* would revolutionize the treatment of human genetic-based diseases. While multiple delivery platforms exist, virus-like particles (VLPs) are one of the most promising. Here, we demonstrated that VLPs can successfully deliver the necessary components for CRISPR-Cas9-mediated homology-directed repair (HDR), albeit at low frequencies. VLPs carrying Cas9 ribonucleoprotein complexes (RNPs) enabled relatively high frequencies of HDR when the

template was delivered to the cells via nucleofection, reaching close to 40% HDR at the highest VLP concentration tested (Fig. 3c). Nucleofection likely delivered a considerable amount of the HDR repair template into the targeted cells' nuclei, suggesting that HDR template delivery is efficiency limiting for VLP-mediated HDR. Although this method requires multiple steps (nucleofection and then VLP transduction) our results suggest that it could be utilized for *ex vivo* genome editing. However, nucleofection is not viable for *in vivo* editing, so we sought to develop methods that would, in principle, allow for *in vivo* editing and that would deliver the Cas9 RNPs and HDR repair templates in one step.

Based on previous work showing that exogenous DNA could be loaded into hepatitis B virus-based VLPs produced from yeast cells (*28*), we reasoned that VLPs derived from 293T cells could be loaded with donor DNA templates via electroporation. As a proof-of-concept, we demonstrated that VLPs could be electroporated with an mNeonGreen-expressing plasmid and could subsequently deliver the plasmid to ~0.4% of a population of treated cells (Fig. 4b). Cas9 VLPs that were loaded with donor DNA through electroporation enabled varying levels of HDR depending on the template used. At the highest concentration tested, VLPs carrying the target strand HDR donor facilitated the highest levels of HDR (Fig. 4c). Previous work has shown that using an asymmetric repair template complementary to the strand not targeted by Cas9 can increase HDR frequencies, because Cas9 asymmetrically releases the cleaved DNA (*11*). Specifically, the protospacer adjacent motif-distal non-target strand is released immediately following cleavage and thus can anneal to short ssDNA donors (*11*). Importantly, electroporation did not appear to affect the ability of VLPs to deliver Cas9 RNPs to cells, as measured by BFP knockout frequencies (Fig. 4c).

Interestingly, following electroporation of VLPs, we observed unexpected aggregates in the solution, suggesting that electroporation led to precipitation of the VLP preparation. We attempted to electroporate VLPs in phosphate-buffered saline (PBS) instead of Opti-MEM, but similar results were observed (data not shown). Different electroporation buffers and conditions clearly needed to be tested to determine whether an electroporation-based protocol could load VLPs with donor DNA templates. Work that built upon the initial experiments presented in this paper suggested nucleofection can load VLPs with HDR repair templates and/or promote associations between the outside of the particle and the DNA (in press, *Cell Reports*). In these experiments, multiple Lonza nucleofection buffers and Nucleofector settings were tested to determine optimal nucleofection conditions. Using these optimal conditions to nucleofect Cas9 VLPs and ssDNA donor templates, Hamilton and colleagues achieved close to 40% HDR in the reporter cell line (in press, *Cell Reports*). The results from our electroporation experiment also suggested that simply mixing VLPs with HDR donors (see "No Electroporation" condition in Fig. 4c) may load VLPs with the templates. Hamilton and colleagues reported similar findings (in press, *Cell Reports*).

Evidently, type of buffer and nucleofection conditions can have a large effect on the efficiency of VLP-enabled Cas9-mediated HDR. Unfortunately, the composition of Lonza nucleofection buffers is proprietary, and we thus can only speculate on the reasons why certain buffers improve the mixing of VLPs and HDR templates. Optimal buffers likely provide positively charged molecules or moieties and reduce repulsive forces between the viral particle and the negatively charged DNA. For instance, to produce VLPs carrying HDR templates, Mangeot and colleagues combined VLPs and copies of a repair template in a solution containing polybrene, which has been shown to promote the formation of glycoprotein and DNA complexes

23

(*24, 27*). Polybrene is cationic and thus could impact the electrostatic interactions between the glycoprotein-pseudotyped particles and the DNA. The buffer used in our electroporation experiments (Opti-MEM or PBS) was likely non-optimal and hence could be one factor that explains the low efficiency of the electroporated VLPs.

Super VLPs packaged both Cas9 RNPs and the lentiviral genome encoding the repair template(s). While Super VLPs could be an attractive all-in-one delivery mechanism, they were ineffective at enabling Cas9-mediated HDR, as negligible levels of HDR were observed when Super VLPs were used to treat the reporter cell line (Fig. 5c). Interestingly, Super VLPs carrying 0 HDR templates showed reduced BFP knockout efficiency compared to Cas9 VLPs, suggesting that the addition of a lentiviral genome to VLPs carrying Cas9 RNPs reduces the efficacy of VLPs. This barrier that arises when packaging both a lentiviral genome and Cas9 RNPs into a VLP must be overcome to produce an all-in-one VLP capable of mediating HDR *in vivo*.

Comparing the results from nucleofection, electroporation, and Super VLP experiments, it appears that there are two major bottlenecks for VLP-enabled Cas9-mediated HDR: the number of repair templates delivered (discussed later) and the delivery of the HDR template to the nucleus. Utilizing recently developed HDR shuttles could address the latter bottleneck. Nguyen and colleagues have developed an HDR "shuttle" that improves the efficiency of CRISPR-Cas9 genome editing (*34*). The HDR template is flanked by truncated Cas9 target sequences such that the Cas9 protein associates with, but does not cleave, the template. Since the Cas9 proteins harbor nuclear localization signals, the HDR template is shuttled to the nucleus. Future work should determine whether Cas9 VLPs can be loaded/associated with HDR shuttles via nucleofection in optimal conditions and whether this strategy would increase HDR efficiency.

<u>Promise and Drawbacks of the Dual-VLP Delivery System</u>

The dual-VLP delivery system showed some promise, as HDR frequencies as close to 1% were achieved (Fig. 6). For this platform to be used in therapeutic settings, the editing efficiency must be increased but perhaps only slightly. It has been hypothesized that editing levels as low as 2-3% can be therapeutic in certain contexts (*35*, *36*), especially if the edited cells proliferate rapidly and exhibit fitness advantages. For example, correction of 3-7% of mutated alleles in liver cells could be therapeutic for individuals with hemophilia B (*36*). Stadtmauer and colleagues used CRISPR-Cas9 to knock out the endogenous TCR and programmed cell death protein 1 in autologous T cells, and using a lentiviral vector, they introduced a cancer-specific TCR transgene into 2-4% of the same T cells. These edited cells were then transferred into patients (*35*). Although this group did not use CRISPR-Cas9 technology to introduce the transgenic TCR, they still showed that relatively low editing frequencies were acceptable in a human clinical trial. Despite the promise of the dual-VLP delivery system, future work must include sequencing to confirm HDR events and to characterize off-target editing. Sequencing can also help determine whether mis-integration of the template occurs when it is delivered as an episome. Canaj and colleagues have surveyed mis-integration events in CRISPR-Cas9-mediated HDR knock-in experiments. They found that using a plasmid HDR donor, which resembles a circular episome, can lead to integration of the plasmid backbone in addition to the desired sequence (*37*).

Increasing the concentration of HDR or Cas9 VLPs did not greatly impact HDR levels (Fig. 6c,d). However, it did appear that increasing the HDR VLP concentration could possibly facilitate higher HDR levels, as, in theory, more copies of the template would be delivered to cells (compare Cas9 VLP + 10X HDR VLP to Cas9 VLP + 2X HDR VLP in Fig. 6d right panel).

Experiments where the concentrations of both VLPs are increased should be performed next. Interestingly, in all of the dual-VLP experiments, we observed some levels of HDR in the HDR VLP Only treatments (between 0.23% and 0.62%), suggesting that HDR can potentially occur in the absence of a Cas9-induced DSB (Fig. 6b-d). However, a relatively few number of cells can skew these frequency measurements; thus, sequencing and more trials must be conducted to determine whether HDR VLPs alone can enable HDR.

While the HDR VLPs were integrase-deficient, Cas9 VLPs contained a functional integrase. However, it is unlikely that the integrase from Cas9 VLPs could integrate the lentiviral genome associated with the HDR VLPs. Previous work has shown that the HIV-1 integrase is tightly associated with viral DNA and RNA as part of the preintegration complex (*38*). This finding would suggest that only the defective integrase from the HDR-VLPs would associate with the transfer genome, effectively precluding integration.

Importantly, it appears that co-transduction with HDR VLPs does not impact the ability for Cas9 VLPs to deliver the RNPs, as the BFP knockout frequency was similar for Cas9 + HDR dual-VLP and Cas9 alone treatments in all experiments (Fig. 6b-d). However, the transduction of two different viral particles that have the same glycoprotein can, in principle, lead to superinfection resistance. In addition to the immune system, superinfection resistance is a viral resistance mechanism used to prevent infection by multiple, similar viruses (*39*). Superinfection resistance occurs when cells chronically infected with one virus are transduced with another virus that uses the same receptor. Following infection with the first virus, the Env protein is expressed in the cell and then binds to its receptor intracellularly, effectively preventing subsequent infections (*40*). In most of the dual-VLP experiments, cells were treated simultaneously with the two VLPs, but superinfection resistance may still apply. VLPs were left

on the treated cells for 3 days before analysis, suggesting that a cell transduced immediately following treatment may not be transducible at later time points even though VLPs were still present. The data do not suggest that infection with HDR VLPs prevents Cas9 VLP infection, but the opposite may hold true, as discussed later.

One considerable drawback of the dual-VLP system is having the repair template be present in double-stranded form and as part of an episome, which can be either circular or linear (*41*). It has been shown that double-stranded donors are less efficient than single-stranded donors for mediating HDR, likely because double-stranded donors have less access to the Cas9 cut site than single stranded donors (*11*). Moreover, Zhang and colleagues demonstrated that HDR efficiency is increased 2- to 5-fold when using a dsDNA HDR donor, compared to a circular plasmid donor (*42*). This group also showed that levels of HDR mediated knock-in were negligible when the homology arms on the circular plasmid donor were less than 300 bp (*42*). The HDR template used in this study had 124 of 127 nucleotides homologous to the native genomic site, and when delivered via a lentiviral genome, the template may have existed on a circular episome. Thus, the relatively low amount of homology and the potentially circular nature of the template could explain the low rate of HDR observed in these experiments.

Another drawback of the dual-VLP system compared to nucleofection is that fewer templates enter the cell. In the nucleofection experiments, we nucleofected 2×10^5 cells with 100 pmol of HDR repair template, which is equivalent to roughly 6×10^{13} copies of the template. Assuming that transfection efficiency was close to 100% and that all nucleofected cells received the same quantity of template, each cell would be delivered with 3×10^8 copies of template. While this calculation is just an estimation and could be orders of magnitude off, it is still clear that HDR VLPs were unable to deliver the same number of templates. Each HDR VLP encoding one

template on the lentiviral genome actually carried two copies of the template because the viral genome exists a dimer of ssRNA (*40*). Although we did not measure the multiplicity of infection (MOI) for the VLPs, we can still make an estimation that illustrates the relatively few number of templates delivered to cells by HDR VLPs. According to the Poisson distribution, even at a high MOI such as 10, only 41% of cells would be infected with more than 10 viral particles (*43*). Thus, assuming an MOI of 10 and high transduction efficiency, the majority of cells transduced with HDR VLPs would have 20 or fewer copies of template. Evidently, VLPs are not able to deliver many copies of an HDR repair template if the template is encoded on the lentiviral genome. VLPs carrying greater numbers of HDR templates are obviously needed in order to improve VLP-mediated HDR.

Several future experiments could seek to address the drawback of having the repair template on a double-stranded episome. First, one could examine the effect of increasing the number of homologous nucleotides on the HDR repair template, as previous work indicated that increasing the amount of homology on a circular piece of DNA increases HDR (*42*). Second, one could attempt to insert Cas9 target sites on either side of the HDR template on the lentiviral genome. Once the lentiviral genome is reverse transcribed and forms an episome in the cell, Cas9 could cleave the episome and release the HDR template. This strategy would potentially allow the template to more freely diffuse in the cell and perhaps increase the frequency of HDR.

Concatenating Multiple Repair Templates on the Lentiviral Genome

By measuring the frequency of mCherry+ cells, we were able to record transduction efficiencies of VLPs carrying a lentiviral genome, and a very interesting trend was observed. For both Super VLPs and HDR VLPs, transduction efficiency decreased as more HDR repair

templates were encoded on the lentiviral genome (Table 2). Previous work that investigated the packaging limit of lentiviral vectors demonstrated that viral titers decreased as the length of the viral vector increased (*44*). Thus, one could argue that the VLP titer and hence the transduction efficiency decreased as the size of the lentiviral genome increased. However, this interpretation is unlikely, as the HDR template is only 127 bp, so adding extra copies of the template onto the genome should not drastically reduce transduction efficiency as we see in the data. Previous work has reported that deletions of tandem repeating sequences in lentiviral vectors can occur during reverse transcription, and thus repeats in lentiviral vectors should be avoided (*45*, *46*). However, it is unclear whether and how deletions of concatenated HDR templates on the lentiviral genome would lead to impaired HDR VLP transduction efficiency.

Interestingly, HDR VLPs, even carrying 2 or 3 templates, have relatively high transduction efficiencies when transduced alone (Table 2). This result would suggest that VLPs packaging a lentiviral genome with concatenated HDR templates can be produced. However, in the dual-VLP system, HDR VLPs with 2 or 3 templates were highly inefficient at transduction (Table 2). This observation could support the possibility of superinfection resistance and imply that viral transduction is compromised in the particles with multiple HDR templates on the genome. If Cas9 VLPs were more efficient at transduction than HDR VLPs, Cas9 VLPs would likely have transduced cells more rapidly following treatment and then potentially have prevented subsequent infection by HDR VLPs.

Nonetheless, given the data, we are unable to definitively determine whether the reduced transduction efficiency is a result of impaired viral production, transduction, or reverse transcription. Further work must be performed to elucidate the part of the viral life cycle that is compromised by having repetitive elements in the lentiviral genome. This work will also help

establish whether our findings are a result of real biological processes or whether they are simply an experimental artifact. That is, any of the engineered components of our delivery system, such as the HIV-1 transfer genome encoding mCherry and HDR repair templates, could contribute to our results. For example, to determine whether VLP production is compromised by having tandem HDR templates on the lentiviral genome, I would perform ELISAs to detect viral protein components (i.e. capsid) and to thus measure viral titers of VLPs packaging concatenated copies of the template on the genome. Then, qPCR could be used to confirm the presence of the lentiviral genome in the budded lentiviral particles. If viral titers decreased as the number of HDR templates increased, we could conclude that VLP production is compromised when templates are concatenated on the genome.

Delivery of New Editing Tools

Our findings showed that VLP-directed Cas9-mediated HDR is possible, but considerably more work needs to be completed to improve efficiency. In the meantime, future studies should elucidate whether VLPs can deliver novel genome editing tools. Cas transposases offer alternative methods to facilitate targeted insertions. Strecker and colleagues have shown that Tn7-like transposons can associate with a CRISPR effector protein and be directed to a specific place in the *Escherichia coli* genome by a CRISPR gRNA (*47*). This RNA-guided DNA transposition occurs 60-66 base pairs downstream of the protospacer and has the potential to be used in therapeutic contexts. While it must be determined whether this editing system is translatable to eukaryotic cells, VLPs could theoretically be used to deliver the proteins, RNA, and DNA necessary for the RNA-guided DNA transposition. In addition to Cas transposases, base and prime editors are other new and exciting CRISPR-Cas-based genome editing tools.

Base editors fuse an enzyme that can interconvert bases to Cas9 nickase, which directs the complex to a site of interest using a sgRNA and cleaves one strand of DNA (*48*, *49*). Base editors can correct any single point mutation. Prime editors mediate targeted insertions, deletions, and all possible single nucleotide conversions without cleaving DNA or needing a donor template (*50*). Future work should consider whether VLPs can successfully deliver base and prime editors. Platforms that enable the efficient and targeted delivery of these new editing tools and the necessary components for CRISPR Cas9-mediated HDR will have an essential role in actualizing the potential of *in vivo* human genome editing.

ACKNOWLEDGEMENTS

REFERENCES

1. J. A. Doudna, The promise and challenge of therapeutic genome editing. *Nature*. **578**, 229–236 (2020).

2. T. Gaj, C. A. Gersbach, C. F. Barbas 3rd, ZFN, TALEN, and CRISPR/Cas-based methods for genome engineering. *Trends Biotechnol*. **31**, 397–405 (2013).

3. F. D. Urnov, J. C. Miller, Y.-L. Lee, C. M. Beausejour, J. M. Rock, S. Augustus, A. C. Jamieson, M. H. Porteus, P. D. Gregory, M. C. Holmes, Highly efficient endogenous human gene correction using designed zinc-finger nucleases. *Nature*. **435**, 646–651 (2005).

4. J. K. Joung, J. D. Sander, TALENs: a widely applicable technology for targeted genome editing. *Nat. Rev. Mol. Cell Biol.* **14**, 49–55 (2013).

5. N. Holt, J. Wang, K. Kim, G. Friedman, X. Wang, V. Taupin, G. M. Crooks, D. B. Kohn, P. D. Gregory, M. C. Holmes, P. M. Cannon, Human hematopoietic stem/progenitor cells modified by zinc-finger nucleases targeted to CCR5 control HIV-1 in vivo. *Nat. Biotechnol.* **28**, 839–847 (2010).

6. L. Poirot, B. Philip, C. Schiffer-Mannioui, D. Le Clerre, I. Chion-Sotinel, S. Derniame, P. Potrel, C. Bas, L. Lemaire, R. Galetto, C. Lebuhotel, J. Eyquem, G. W.-K. Cheung, A. Duclert, A. Gouble, S. Arnould, K. Peggs, M. Pule, A. M. Scharenberg, J. Smith, Multiplex Genome-Edited T-cell Manufacturing Platform for "Off-the-Shelf" Adoptive T-cell Immunotherapies. *Cancer Res.* **75**, 3853–3864 (2015).

7. A. V. Wright, J. K. Nuñez, J. A. Doudna, Biology and Applications of CRISPR Systems: Harnessing Nature's Toolbox for Genome Engineering. *Cell*. **164**, 29–44 (2016).

8. M. Jinek, K. Chylinski, I. Fonfara, M. Hauer, J. A. Doudna, E. Charpentier, A Programmable Dual-RNA-Guided DNA Endonuclease in Adaptive Bacterial Immunity. *Science*. **337** (2012), pp. 816–821.

9. C. D. Yeh, C. D. Richardson, J. E. Corn, Advances in genome editing through control of DNA repair pathways. *Nat. Cell Biol.* **21**, 1468–1478 (2019).

10. V. T. Chu, C. Van Trung, T. Weber, B. Wefers, W. Wurst, S. Sander, K. Rajewsky, R. Kühn, Increasing the efficiency of homology-directed repair for CRISPR-Cas9-induced precise gene editing in mammalian cells. *Nature Biotechnology*. **33** (2015), pp. 543–548.

11. C. D. Richardson, G. J. Ray, M. A. DeWitt, G. L. Curie, J. E. Corn, Enhancing homology-directed genome editing by catalytically active and inactive CRISPR-Cas9 using asymmetric donor DNA. *Nat. Biotechnol.* **34**, 339–344 (2016).

12. H. Frangoul, D. Altshuler, M. D. Cappellini, Y.-S. Chen, J. Domm, B. K. Eustace, J. Foell, J. de la Fuente, S. Grupp, R. Handgretinger, T. W. Ho, A. Kattamis, A. Kernytsky, J. Lekstrom-Himes, A. M. Li, F. Locatelli, M. Y. Mapara, M. de Montalembert, D. Rondelli, A. Sharma, S. Sheth, S. Soni, M. H. Steinberg, D. Wall, A. Yen, S. Corbacioglu,

CRISPR-Cas9 Gene Editing for Sickle Cell Disease and β-Thalassemia. *N. Engl. J. Med.* **384**, 252–260 (2021).

13. R. C. Wilson, L. A. Gilbert, The Promise and Challenge of In Vivo Delivery for Genome Therapeutics. *ACS Chem. Biol.* **13**, 376–382 (2018).

14. M. Tabebordbar, K. Zhu, J. K. W. Cheng, W. L. Chew, J. J. Widrick, W. X. Yan, C. Maesner, E. Y. Wu, R. Xiao, F. A. Ran, L. Cong, F. Zhang, L. H. Vandenberghe, G. M. Church, A. J. Wagers, In vivo gene editing in dystrophic mouse muscle and muscle stem cells. *Science*. **351**, 407–411 (2016).

15. M. L. Maeder, M. Stefanidakis, C. J. Wilson, R. Baral, L. A. Barrera, G. S. Bounoutas, D. Bumcrot, H. Chao, D. M. Ciulla, J. A. DaSilva, A. Dass, V. Dhanapal, T. J. Fennell, A. E. Friedland, G. Giannoukos, S. W. Gloskowski, A. Glucksmann, G. M. Gotta, H. Jayaram, S. J. Haskett, B. Hopkins, J. E. Horng, S. Joshi, E. Marco, R. Mepani, D. Reyon, T. Ta, D. G. Tabbaa, S. J. Samuelsson, S. Shen, M. N. Skor, P. Stetkiewicz, T. Wang, C. Yudkoff, V. E. Myer, C. F. Albright, H. Jiang, Development of a gene-editing approach to restore vision loss in Leber congenital amaurosis type 10. *Nat. Med.* **25**, 229–233 (2019).

16. First CRISPR therapy dosed. *Nat. Biotechnol.* **38**, 382 (2020).

17. Y. Yang, L. Wang, P. Bell, D. McMenamin, Z. He, J. White, H. Yu, C. Xu, H. Morizono, K. Musunuru, M. L. Batshaw, J. M. Wilson, A dual AAV system enables the Cas9-mediated correction of a metabolic liver disease in newborn mice. *Nat. Biotechnol.* **34**, 334–338 (2016).

18. F. A. Ran, L. Cong, W. X. Yan, D. A. Scott, J. S. Gootenberg, A. J. Kriz, B. Zetsche, O. Shalem, X. Wu, K. S. Makarova, E. V. Koonin, P. A. Sharp, F. Zhang, In vivo genome editing using Staphylococcus aureus Cas9. *Nature*. **520**, 186–191 (2015).

19. A. E. Friedland, R. Baral, P. Singhal, K. Loveluck, S. Shen, M. Sanchez, E. Marco, G. M. Gotta, M. L. Maeder, E. M. Kennedy, A. V. R. Kornepati, A. Sousa, M. A. Collins, H. Jayaram, B. R. Cullen, D. Bumcrot, Characterization of Staphylococcus aureus Cas9: a smaller Cas9 for all-in-one adeno-associated virus delivery and paired nickase applications. *Genome Biol.* **16**, 257 (2015).

20. M. Wang, J. A. Zuris, F. Meng, H. Rees, S. Sun, P. Deng, Y. Han, X. Gao, D. Pouli, Q. Wu, I. Georgakoudi, D. R. Liu, Q. Xu, Efficient delivery of genome-editing proteins using bioreducible lipid nanoparticles. *Proc. Natl. Acad. Sci. U. S. A.* **113**, 2868–2873 (2016).

21. J. D. Finn, A. R. Smith, M. C. Patel, L. Shaw, M. R. Youniss, J. van Heteren, T. Dirstine, C. Ciullo, R. Lescarbeau, J. Seitzer, R. R. Shah, A. Shah, D. Ling, J. Growe, M. Pink, E. Rohde, K. M. Wood, W. E. Salomon, W. F. Harrington, C. Dombrowski, W. R. Strapps, Y. Chang, D. V. Morrissey, A Single Administration of CRISPR/Cas9 Lipid Nanoparticles Achieves Robust and Persistent In Vivo Genome Editing. *Cell Rep.* **22**, 2227–2235 (2018).

22. H. Yin, C.-Q. Song, J. R. Dorkin, L. J. Zhu, Y. Li, Q. Wu, A. Park, J. Yang, S. Suresh, A. Bizhanova, A. Gupta, M. F. Bolukbasi, S. Walsh, R. L. Bogorad, G. Gao, Z. Weng, Y. Dong,

V. Koteliansky, S. A. Wolfe, R. Langer, W. Xue, D. G. Anderson, Therapeutic genome editing by combined viral and non-viral delivery of CRISPR system components in vivo. *Nat. Biotechnol.* **34**, 328–333 (2016).

23. S. J. Kaczmarczyk, K. Sitaraman, H. A. Young, S. H. Hughes, D. K. Chatterjee, Protein delivery using engineered virus-like particles. *Proc. Natl. Acad. Sci. U. S. A.* **108**, 16998–17003 (2011).

24. P. E. Mangeot, V. Risson, F. Fusil, A. Marnef, E. Laurent, J. Blin, V. Mournetas, E. Massouridès, T. J. M. Sohier, A. Corbin, F. Aubé, M. Teixeira, C. Pinset, L. Schaeffer, G. Legube, F.-L. Cosset, E. Verhoeyen, T. Ohlmann, E. P. Ricci, Genome editing in primary cells and in vivo using viral-derived Nanoblades loaded with Cas9-sgRNA ribonucleoproteins. *Nature Communications*. **10** (2019), , doi:10.1038/s41467-018-07845-z.

25. S. Kim, D. Kim, S. W. Cho, J. Kim, J.-S. Kim, Highly efficient RNA-guided genome editing in human cells via delivery of purified Cas9 ribonucleoproteins. *Genome Research*. **24** (2014), pp. 1012–1019.

26. K. Schumann, S. Lin, E. Boyer, D. R. Simeonov, M. Subramaniam, R. E. Gate, G. E. Haliburton, C. J. Ye, J. A. Bluestone, J. A. Doudna, A. Marson, Generation of knock-in primary human T cells using Cas9 ribonucleoproteins. *Proc. Natl. Acad. Sci. U. S. A.* **112**, 10437–10442 (2015).

27. T. Okimoto, T. Friedmann, A. Miyanohara, VSV-G envelope glycoprotein forms complexes with plasmid DNA and MLV retrovirus-like particles in cell-free conditions and enhances DNA transfection. *Mol. Ther.* **4**, 232–238 (2001).

28. T. Yamada, Y. Iwasaki, H. Tada, H. Iwabuki, M. K. L. Chuah, T. VandenDriessche, H. Fukuda, A. Kondo, M. Ueda, M. Seno, K. Tanizawa, S. 'ichi Kuroda, Nanoparticles for the delivery of genes and drugs to human hepatocytes. *Nat. Biotechnol.* **21**, 885–890 (2003).

29. A. Glaser, B. McColl, J. Vadolas, GFP to BFP Conversion: A Versatile Assay for the Quantification of CRISPR/Cas9-mediated Genome Editing. *Mol. Ther. Nucleic Acids*. **5**, e334 (2016).

30. E. O. Freed, HIV-1 assembly, release and maturation. *Nat. Rev. Microbiol.* **13**, 484–496 (2015).

31. E. Schmider, M. Ziegler, E. Danay, L. Beyer, M. Bühner, Is it really robust? Reinvestigating the robustness of ANOVA against violations of the normal distribution assumption. *Methodology* . **6**, 147–151 (2010).

32. M. J. Blanca, R. Alarcón, J. Arnau, R. Bono, R. Bendayan, Non-normal data: Is ANOVA still a valid option? *Psicothema*. **29**, 552–557 (2017).

33. M. J. Blanca, R. Alarcón, J. Arnau, R. Bono, R. Bendayan, Effect of variance ratio on ANOVA robustness: Might 1.5 be the limit? *Behav. Res. Methods*. **50**, 937–962 (2018).

34. D. N. Nguyen, T. L. Roth, P. J. Li, P. A. Chen, R. Apathy, M. R. Mamedov, L. T. Vo, V. R. Tobin, D. Goodman, E. Shifrut, J. A. Bluestone, J. M. Puck, F. C. Szoka, A. Marson, Polymer-stabilized Cas9 nanoparticles and modified repair templates increase genome editing efficiency. *Nat. Biotechnol.* **38**, 44–49 (2020).

35. E. A. Stadtmauer, J. A. Fraietta, M. M. Davis, A. D. Cohen, K. L. Weber, E. Lancaster, P. A. Mangan, I. Kulikovskaya, M. Gupta, F. Chen, L. Tian, V. E. Gonzalez, J. Xu, I.-Y. Jung, J. Joseph Melenhorst, G. Plesa, J. Shea, T. Matlawski, A. Cervini, A. L. Gaymon, S. Desjardins, A. Lamontagne, J. Salas-Mckee, A. Fesnak, D. L. Siegel, B. L. Levine, J. K. Jadlowsky, R. M. Young, A. Chew, W.-T. Hwang, E. O. Hexner, B. M. Carreno, C. L. Nobles, F. D. Bushman, K. R. Parker, Y. Qi, A. T. Satpathy, H. Y. Chang, Y. Zhao, S. F. Lacey, C. H. June, CRISPR-engineered T cells in patients with refractory cancer. *Science.* **367** (2020), doi:10.1126/science.aba7365.

36. D. B. T. Cox, R. J. Platt, F. Zhang, Therapeutic genome editing: prospects and challenges. *Nat. Med.* **21**, 121–131 (2015).

37. H. Canaj, J. A. Hussmann, H. Li, K. A. Beckman, L. Goodrich, N. H. Cho, Y. J. Li, D. A. Santos, A. McGeever, E. M. Stewart, V. Pessino, M. A. Mandegar, C. Huang, L. Gan, B. Panning, B. Huang, J. S. Weissman, M. D. Leonetti, Deep profiling reveals substantial heterogeneity of integration outcomes in CRISPR knock-in experiments. *bioRxiv* (2019), p. 841098.

38. M. I. Bukrinsky, N. Sharova, T. L. McDonald, T. Pushkarskaya, W. G. Tarpley, M. Stevenson, Association of integrase, matrix, and reverse transcriptase antigens of human immunodeficiency virus type 1 with viral nucleic acids following acute infection. *Proc. Natl. Acad. Sci. U. S. A.* **90**, 6125–6129 (1993).

39. M. Nethe, B. Berkhout, A. C. van der Kuyl, Retroviral superinfection resistance. *Retrovirology.* **2**, 52 (2005).

40. S. P. Goff, in *Fields Virology*, D. M. Knipe & P. M. Howley, Eds. (Lippincott, Williams & Wilkins, Philadelphia, 6th ed., 2013), pp. 1424–1473.

41. M. B. Banasik, P. B. McCray Jr, Integrase-defective lentiviral vectors: progress and applications. *Gene Ther.* **17**, 150–157 (2010).

42. J.-P. Zhang, X.-L. Li, G.-H. Li, W. Chen, C. Arakaki, G. D. Botimer, D. Baylink, L. Zhang, W. Wen, Y.-W. Fu, J. Xu, N. Chun, W. Yuan, T. Cheng, X.-B. Zhang, Efficient precise knockin with a double cut HDR donor after CRISPR/Cas9-mediated double-stranded DNA cleavage. *Genome Biol.* **18**, 35 (2017).

43. R. C. Condit, in *Fields Virology*, D. M. Knipe & P. M. Howley, Eds. (Lippincott, Williams & Wilkins, Philadelphia, 6th ed., 2013), pp. 21–51.

44. M. Kumar, B. Keller, N. Makalou, R. E. Sutton, Systematic determination of the packaging limit of lentiviral vectors. *Hum. Gene Ther.* **12**, 1893–1905 (2001).

45. F. Urusov, D. Glazkova, D. Omelchenko, E. Bogoslovskaya, G. Tsyganova, K. Kersting, G. Shipulin, V. Pokrovsky, Optimization of Polycistronic Anti-CCR5 Artificial microRNA Leads to Improved Accuracy of Its Lentiviral Vector Transfer and More Potent Inhibition of HIV-1 in CD4+ T-Cells. *Cells*. **7**, 10 (2018).

46. B. W. Rhode, M. Emerman, H. M. Temin, Instability of large direct repeats in retrovirus vectors. *J. Virol.* **61**, 925–927 (1987).

47. J. Strecker, A. Ladha, Z. Gardner, J. L. Schmid-Burgk, K. S. Makarova, E. V. Koonin, F. Zhang, RNA-guided DNA insertion with CRISPR-associated transposases. *Science*. **365**, 48–53 (2019).

48. A. C. Komor, Y. B. Kim, M. S. Packer, J. A. Zuris, D. R. Liu, Programmable editing of a target base in genomic DNA without double-stranded DNA cleavage. *Nature*. **533**, 420–424 (2016).

49. N. M. Gaudelli, A. C. Komor, H. A. Rees, M. S. Packer, A. H. Badran, D. I. Bryson, D. R. Liu, Programmable base editing of A•T to G•C in genomic DNA without DNA cleavage. *Nature*. **551**, 464–471 (2017).

50. A. V. Anzalone, P. B. Randolph, J. R. Davis, A. A. Sousa, L. W. Koblan, J. M. Levy, P. J. Chen, C. Wilson, G. A. Newby, A. Raguram, D. R. Liu, Search-and-replace genome editing without double-strand breaks or donor DNA. *Nature*. **576**, 149–157 (2019).

Table 1. Names, descriptions and sources of plasmids.

Plasmid Name	Description	Source
VSV-G	Encodes the VSV-G glycoprotein	addgene.org/8454/
Gag-Pol (psPax2)	Contains the HIV-1 *gag* and *pol* genes	addgene.org/12260/
psPax2-D64V	Identical to psPax2 plasmid but contains a mutation in the integrase portion of the *pol* gene	addgene.org/63586/
Gag-Cas9	Sequence encoding the *Streptococcus pyogenes* Cas9 protein is fused to the *gag* gene	This study
sgRNA	Encodes a specific sgRNA sequence that is under the control of the U6 promoter	This study
Transfer Genome	Encodes the HDR template(s) and harbors the gene encoding mCherry in between long terminal repeats	addgene.org/121669/
mNeonGreen	Cells containing this plasmid express mNeonGreen	Allele Biotechnology
GFP	Encodes the GFP protein	Lonza

Table 2. mCherry+ frequency (mean ± SD) in cells transduced with VLPs carrying a lentiviral genome that encoded mCherry.

# HDR Templates[a]	Super VLP[b] (n=2)	HDR VLP[c] with Cas9 VLP (n=3)[d]	HDR VLP[c] Alone (n=1)
0	94.10 ± 0.71	97.43 ± 0.84	99.5
1	74.25 ± 3.75	92.4 ± 2.34	99.6
2	4.855 ± 0.42	35.73 ± 1.42	88.9
3	2.61 ± 0.30	18.07 ± 1.99	77.8

[a]The HIV-1 lentiviral genome encoded 0-3 copies of the HDR template.
[b]Super VLPs (5X concentrated) co-packaged Cas9 RNPs and a lentiviral genome.
[c]HDR VLPs (2X concentrated) delivered just the lentiviral genome.
[d]All pairwise comparisons of mCherry+ frequency between different conditions were significantly different ($p<0.05$).

Figure 1a.
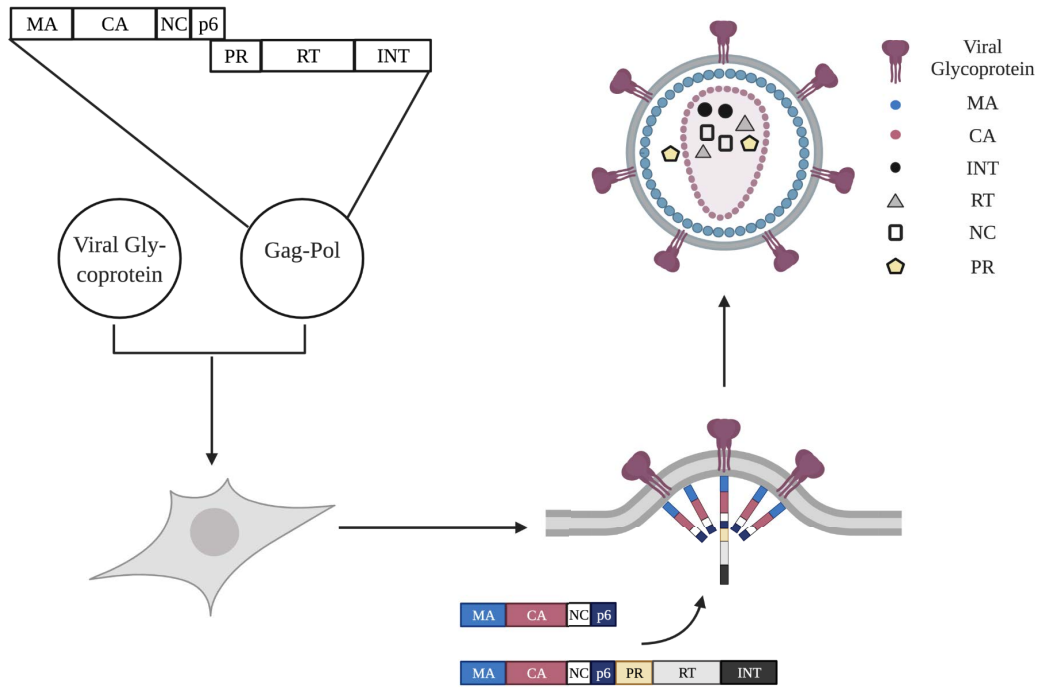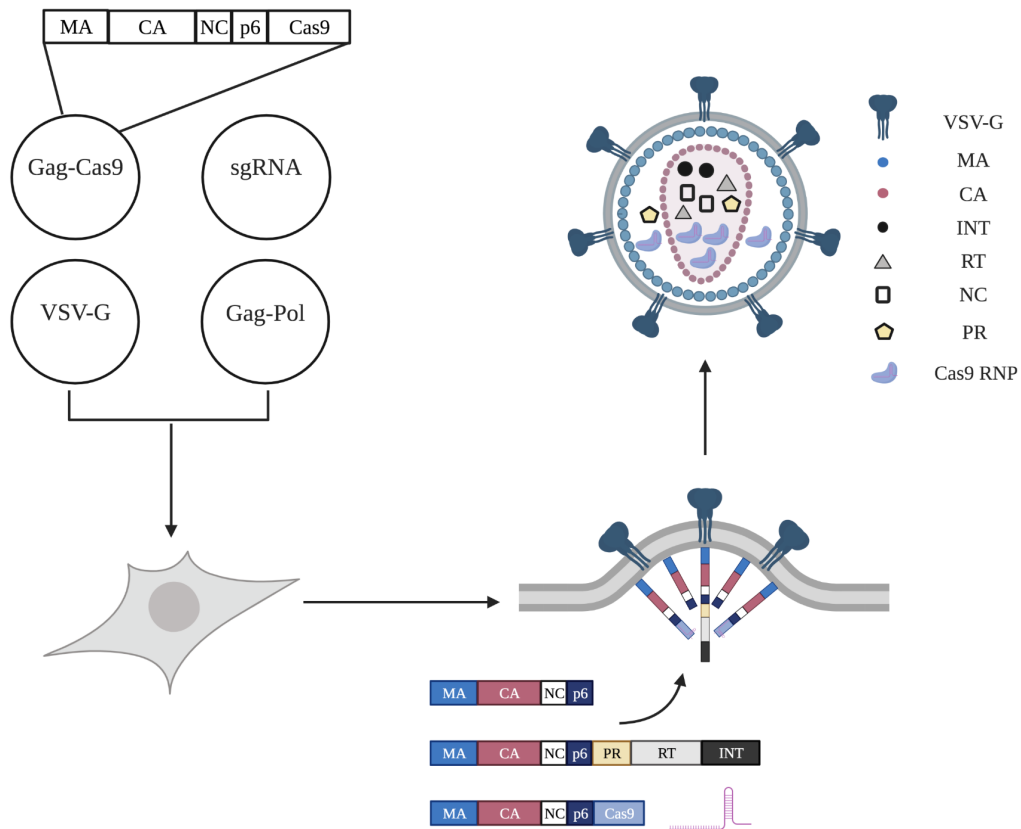
Figure 1. Lenti-X 293T cells transfected with specific plasmids produce VLPs. **a**, Lenti-X 293T cells transfected with two plasmids will produce pseudotyped VLPs. One plasmid encodes the viral glycoprotein and the second plasmid encodes the HIV-1 *gag* and *pol* genes. Following transfection, the Gag and Gag-Pol polyproteins are produced and then packaged into a budding VLP. Once the VLP is released from the cell, HIV-1 proteases cleave the polyproteins to release the individual proteins. **b**, In this study, Lenti-X 293T cells were transfected with four plasmids to produce VLPs carrying Cas9 RNPs. In addition to the plasmid encoding the VSV-G glycoprotein and the Gag-Pol plasmid, two other plasmids were used. The Gag-Cas9 plasmid encodes the Gag polyprotein fused to the Cas9 protein, and the final plasmid encodes a sgRNA that directs the Cas9 protein to the site of interest. Once transcribed, the sgRNA associates with the Cas9 portion of the Gag-Cas9 fusion polyprotein. The Gag-Cas9 polyproteins are then packaged into budding VLPs, and HIV-1 proteases cleave the polyproteins to release the Cas9 RNPs. MA, matrix; CA, capsid; NC, nucleocapsid; PR, protease; INT, integrase; RT, reverse transcriptase.
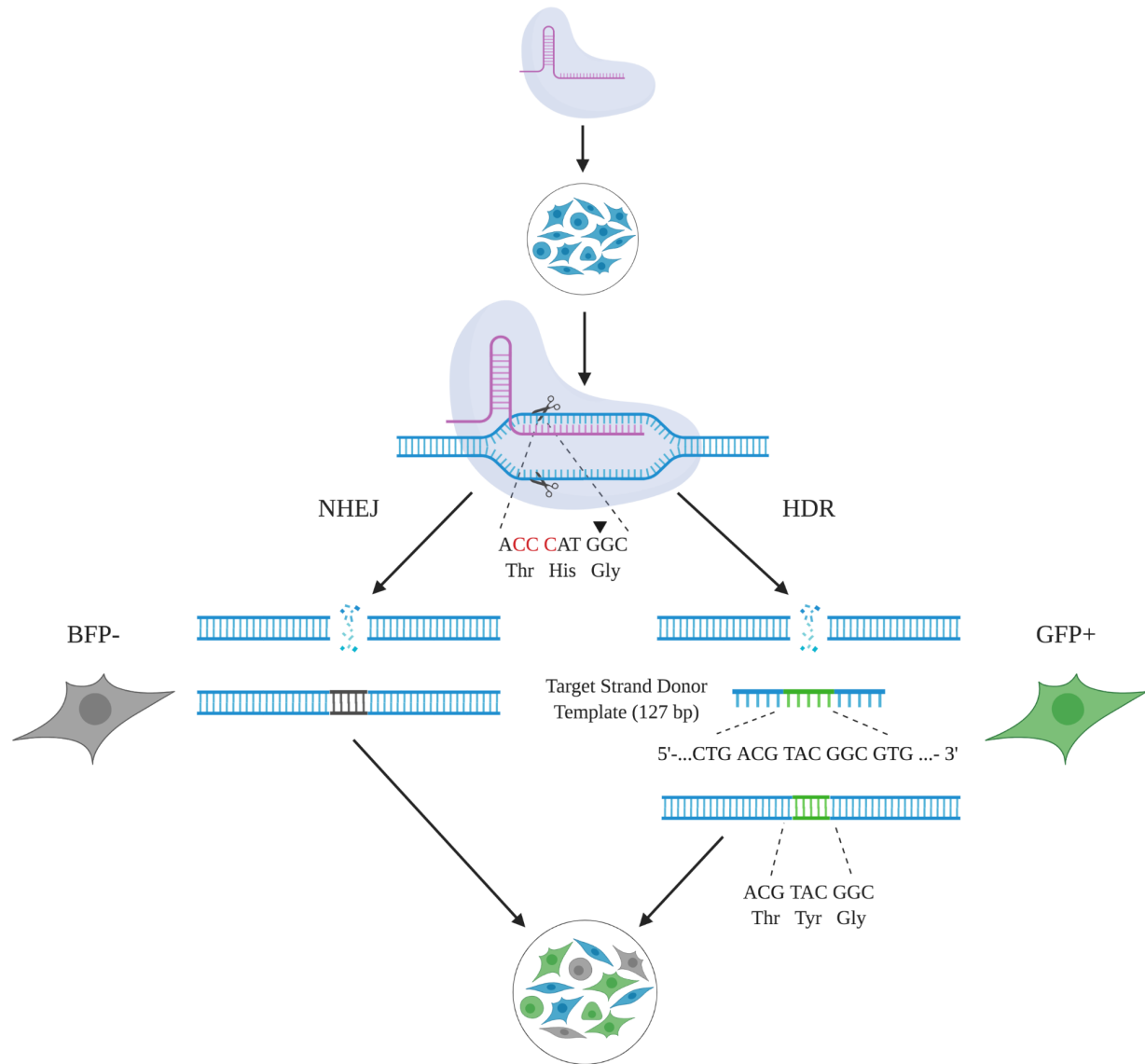
Figure 2. Overview of the BFP-to-GFP reporter cell line used to record HDR frequencies. The *BFP* gene in the BFP reporter cell line was targeted by Cas9 RNPs. Upon Cas9-mediated cleavage, the double-stranded break could be repaired via non-homologous end joining (NHEJ), causing knockout of the *BFP* gene. Alternatively, if a donor DNA template was provided, homology directed repair (HDR) could occur. The donor template used in these experiments instigated three base-pair conversions that, together, destroyed the PAM sequence (shown in red) and caused the cell to produce GFP instead of BFP. Thus, in the treated population of cells, those that underwent HDR (GFP+) could be distinguished from those that underwent NHEJ (BFP+) and from wild-type/unedited cells (BFP+). Adapted from (Richardson et al. 2016).

Figure 3a.

Cas9 VLP
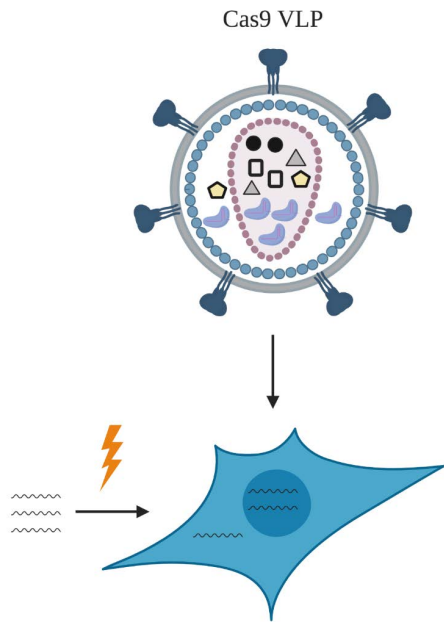
b.
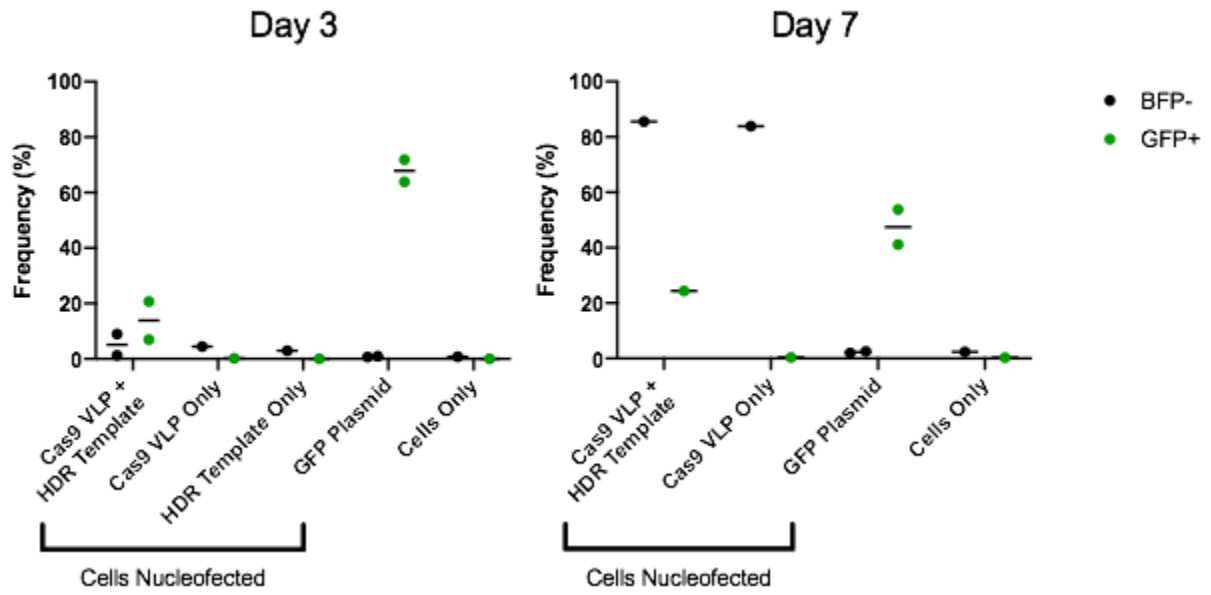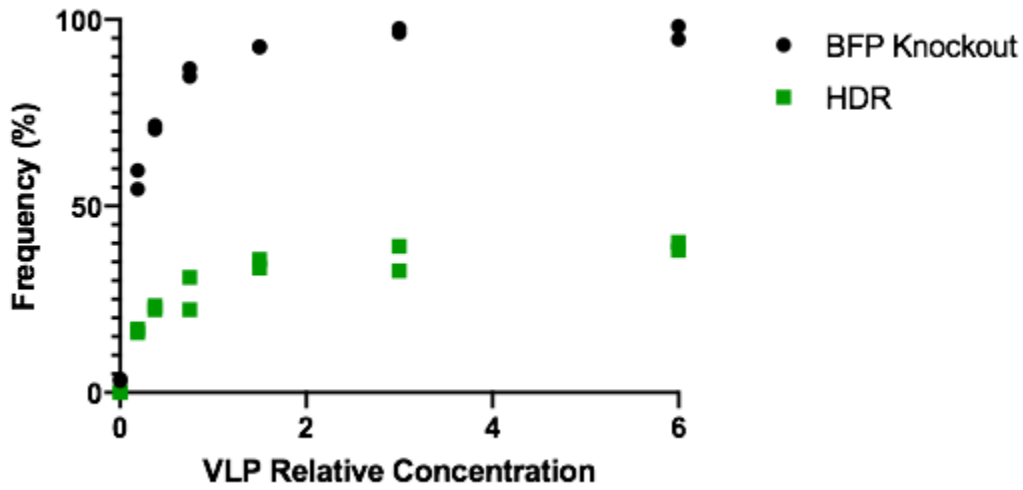
Figure 3c.

d.
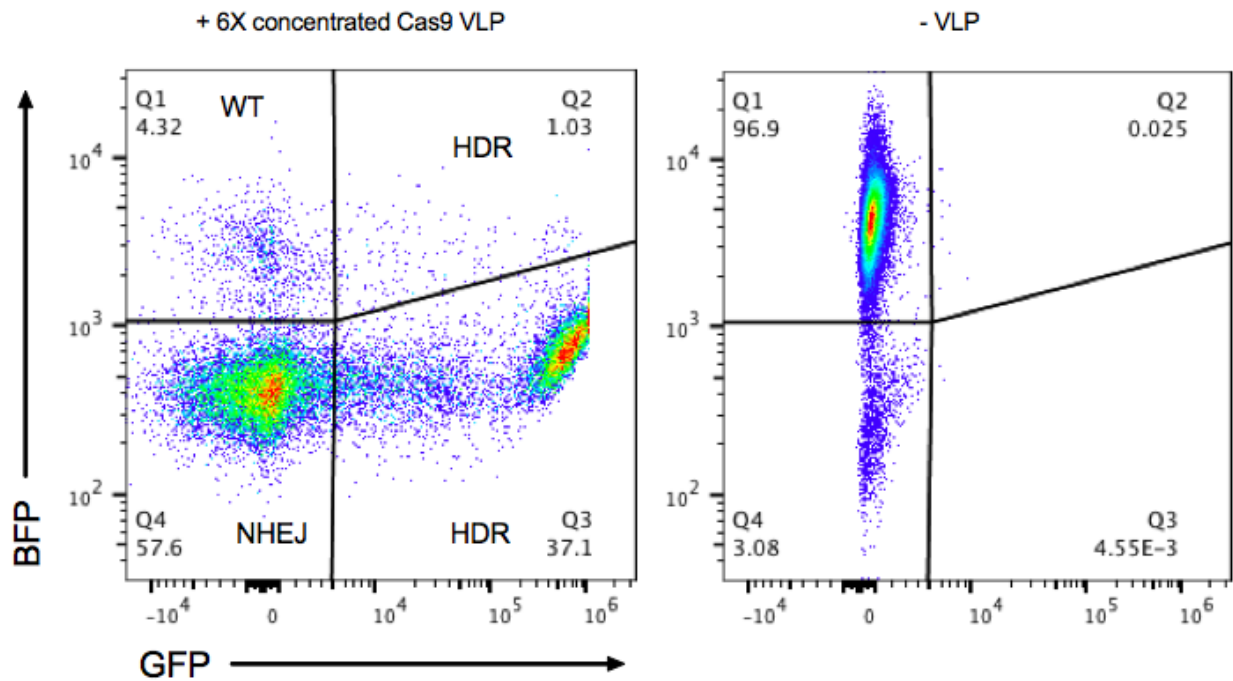
Figure 3. VLPs carrying Cas9 RNPs enabled Cas9-mediated HDR when the donor template was nucleofected into cells. **a**, BFP 293T cells were nucleofected with the HDR template and then transduced with VLPs carrying anti-*BFP* Cas9 RNPs ("Cas9 VLPs"). **b**, Frequency of BFP- and GFP+ cells (percentage of cells in transduced population) 3 and 7 days post-transduction with anti-*BFP* Cas9 VLPs and post-nucleofection with template or control plasmid (n=2 or 1). Cell populations were treated with 0.6X concentrated VLPs. The median for each treatment is shown as a horizontal bar. **c**, BFP knockout and HDR frequencies in cell populations 7 days post-nucleofection and post-transduction with anti-*BFP* Cas9 VLPs at different concentrations

(n=2). Relative VLP concentration is an arbitrary concentration metric. VLPs produced by Lenti-X cells in one 100 mm plate and resuspended in 1mL of Opti-MEM following ultracentrifugation are 1X concentrated. The 0X concentrated treatment corresponded to cells nucleofected with the HDR template but not transduced with VLPs. BFP knockout frequency was quantified by summing Q3 and Q4, and HDR frequency was quantified by summing Q2 and Q3, as shown in (**d**). For (**b**) and (**c**), each data point represents one population of treated cells, and each cell population is represented twice in each graph, once according to the percentage of BFP- cells in the population and once according to the percentage of GFP+ cells in the population. **d**, Representative flow cytometry plots from (**c**) showing three different cell populations. WT, wild-type; NHEJ, nonhomologous end joining; HDR, homology directed repair.

Figure 4a.
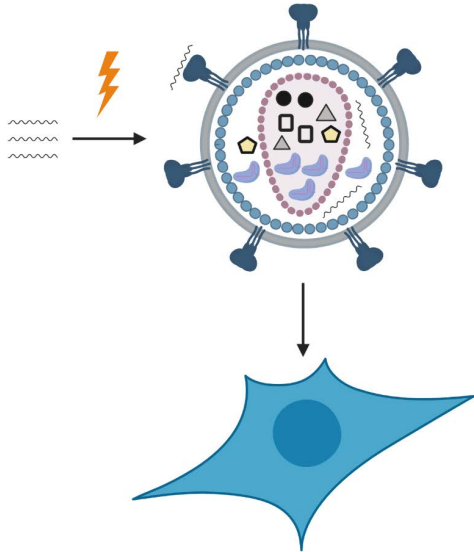
b.
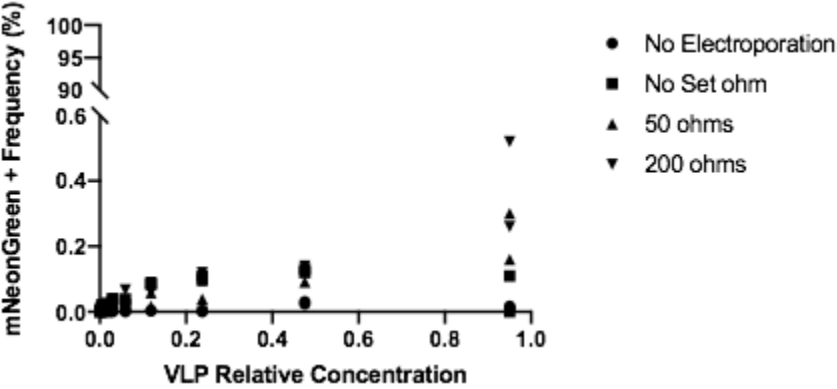
Figure 4c.
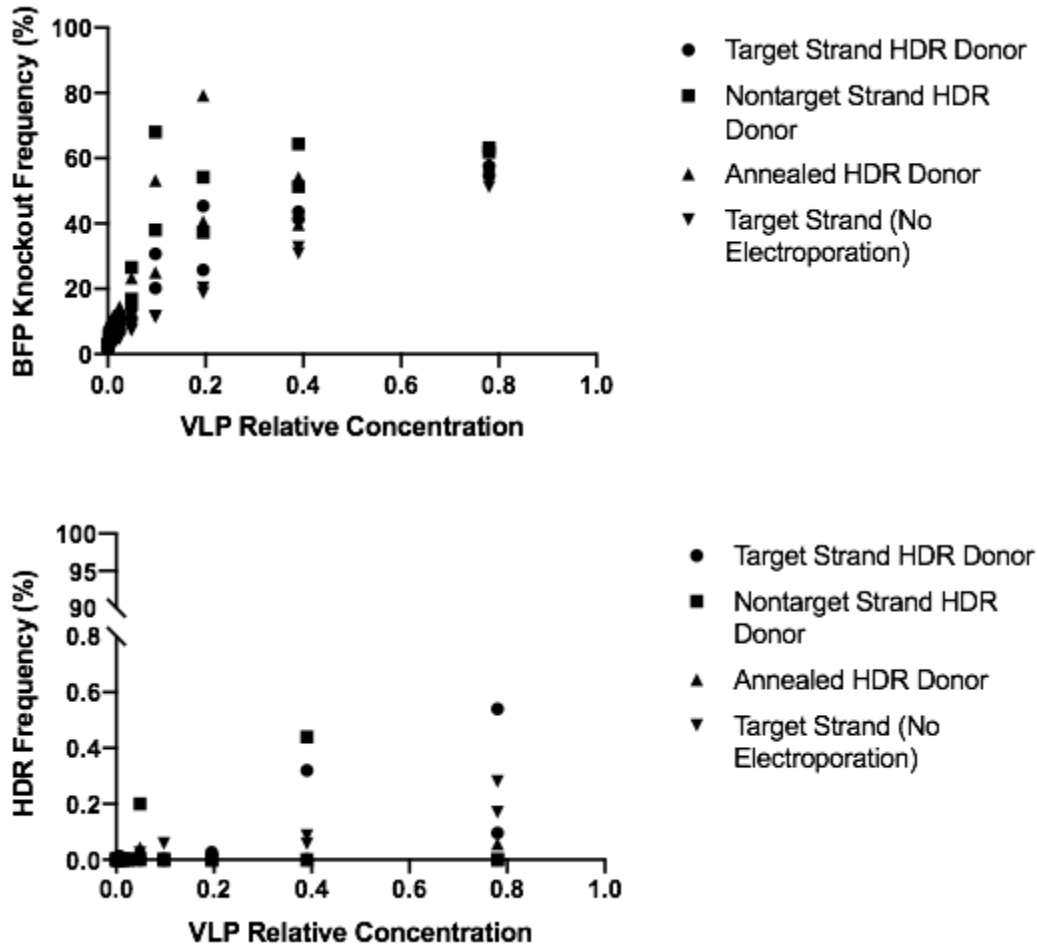
Figure 4. VLPs electroporated with a donor DNA template were able to deliver the necessary components for Cas9-mediated HDR. **a**, VLPs carrying Cas9 RNPs were electroporated with HDR repair templates. BFP 293T cells were then treated with the electroporated VLPs. **b**, Frequency of mNeonGreen+ cells in populations transduced with anti-*B2M* Cas9 VLPs that were electroporated with an mNeonGreen plasmid at different resistances (n=2). VLPs were electroporated at a random resistance in the "No Set ohm" condition. Data were collected 3 days post-transduction. **c**, BFP knockout and HDR frequencies in cell populations 7 days after treatment with anti-*BFP* Cas9 VLPs that were electroporated with different HDR templates (n=2). VLP relative concentration is an arbitrary concentration metric. VLPs produced by Lenti-X cells in one 100 mm plate and resuspended in 1mL of Opti-MEM following ultracentrifugation are 1X concentrated. The 0X concentrated treatment corresponded to cells that were not transduced with VLPs. Each data point represents one population of treated cells, and in (**c**), each cell population is represented twice across the two graphs, once according to the percentage of BFP- cells in the population and once according to the percentage of HDR+ cells in the population.
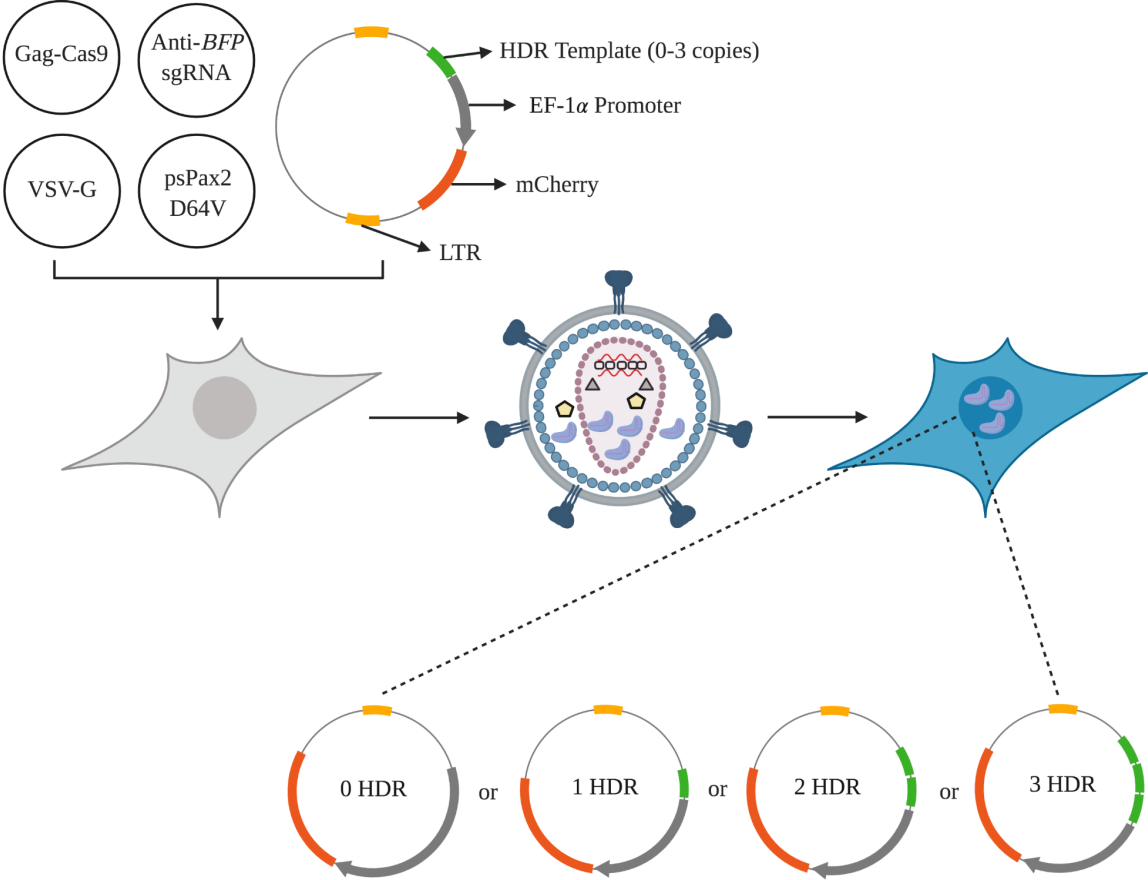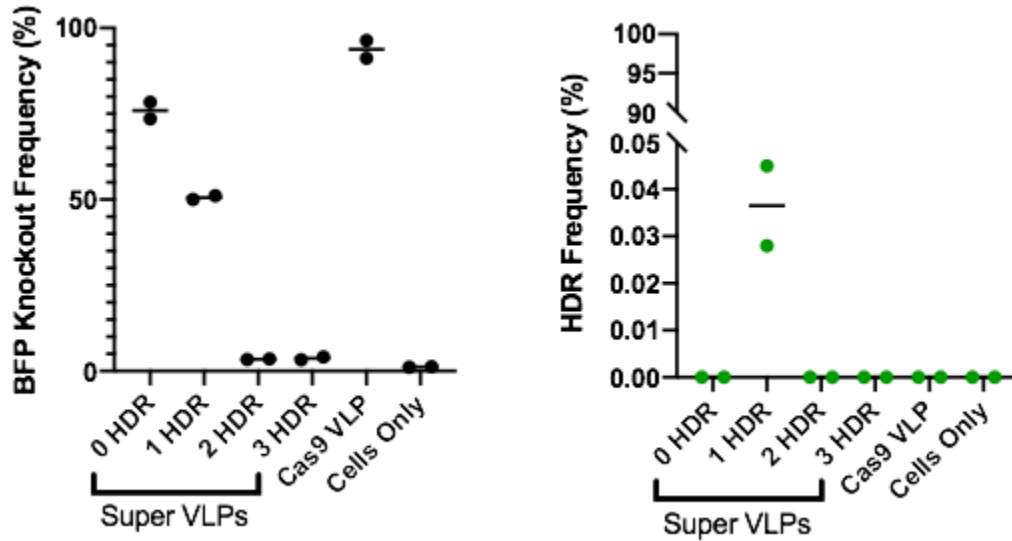
Figure 5a.

Super VLP

b.

Gag-Cas9

Anti-*BFP* sgRNA

VSV-G

psPax2 D64V

HDR Template (0-3 copies)

EF-1α Promoter

mCherry

LTR

0 HDR   or   1 HDR   or   2 HDR   or   3 HDR
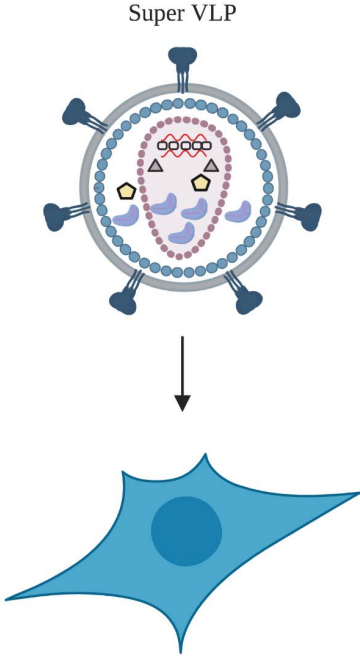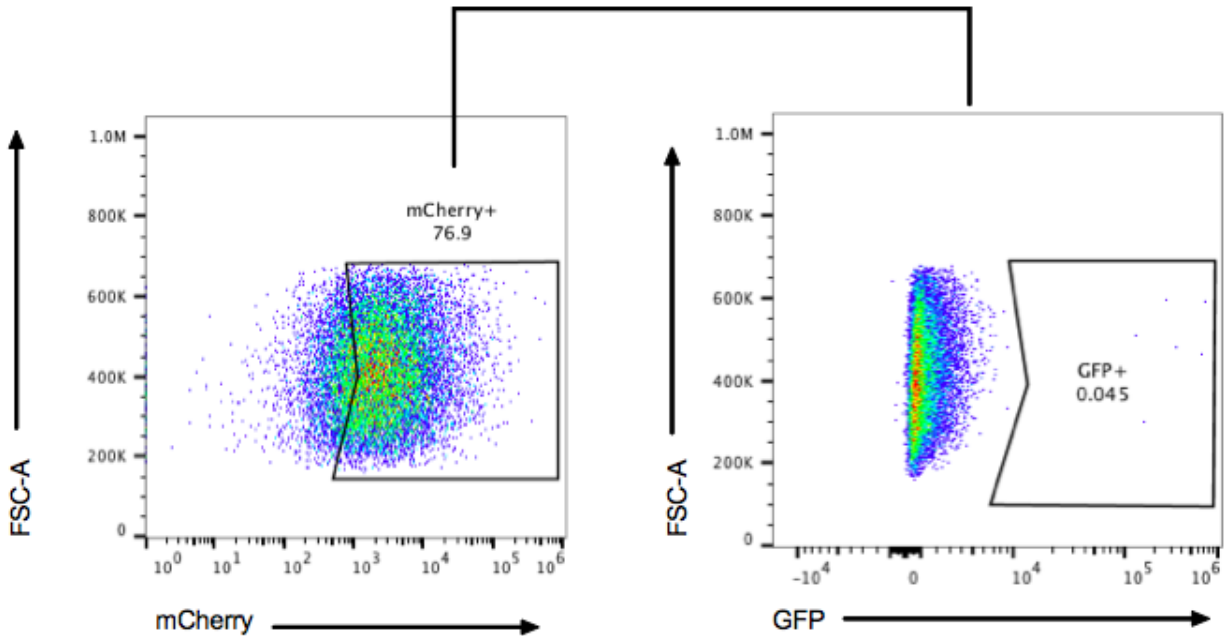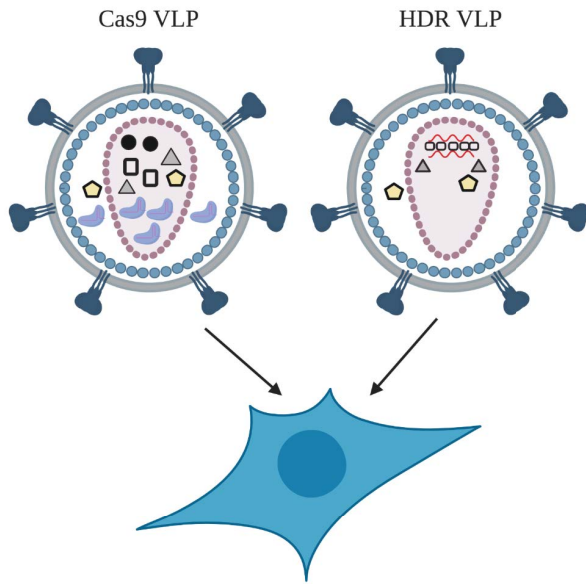
Figure 5c.

d.

Figure 5. "Super VLPs" carrying Cas9 RNPs and the lentiviral genome that encoded one HDR template facilitated very low levels of Cas9-induced HDR. **a**, Integrase-defective VLPs were packaged with anti-*BFP* Cas9 RNPs and a lentiviral genome encoding the HDR template(s). BFP 239T cells were then treated with these Super VLPs. In the diagram, the integrase symbol (●) is omitted to demonstrate that these VLPs were integrase-defective. **b**, LentiX cells were transfected with a plasmid encoding the HDR template(s) in between long terminal repeats

(LTRs) in addition to the plasmids necessary to generate Cas9 VLPs. The transfer genome plasmid also carried the *mCherry* gene, which was under the control of the EF-1α promoter. The lentiviral genome forms an episome in the cell because of the absence of functional integrase. This episome can be circular or linear. One kind of a circular episome is shown here. **c**, BFP knockout and HDR frequencies in cell populations 7 days after transduction with Super VLPs carrying a lentiviral genome that encoded 0 to 3 copies of the HDR template (n=2). All VLPs were 5X concentrated. The median for each treatment is shown as a horizontal bar. Each data point represents one population of treated cells, and each cell population is represented twice across the two graphs, once according to the percentage of BFP- cells in the population and once according to the percentage of HDR+ cells in the population. **d**, Gating scheme to quantify cells that underwent HDR. For the experiments in which the donor template was encoded on the lentiviral genome, mCherry+/GFP+ cells were identified as HDR+ cells.
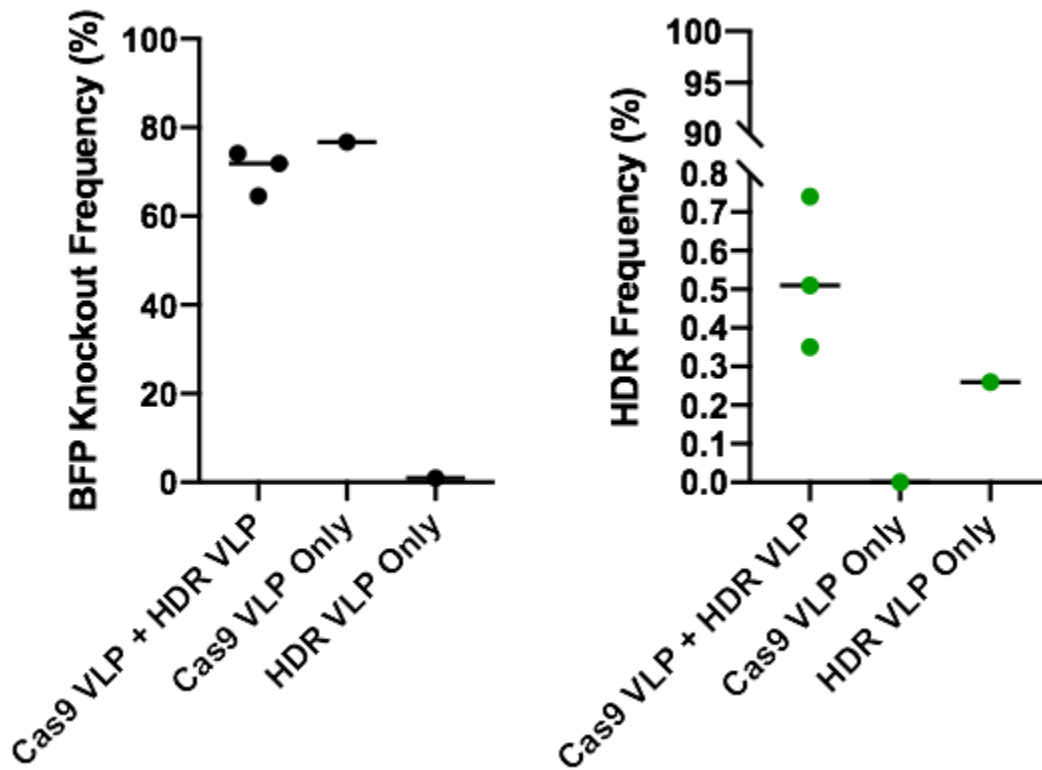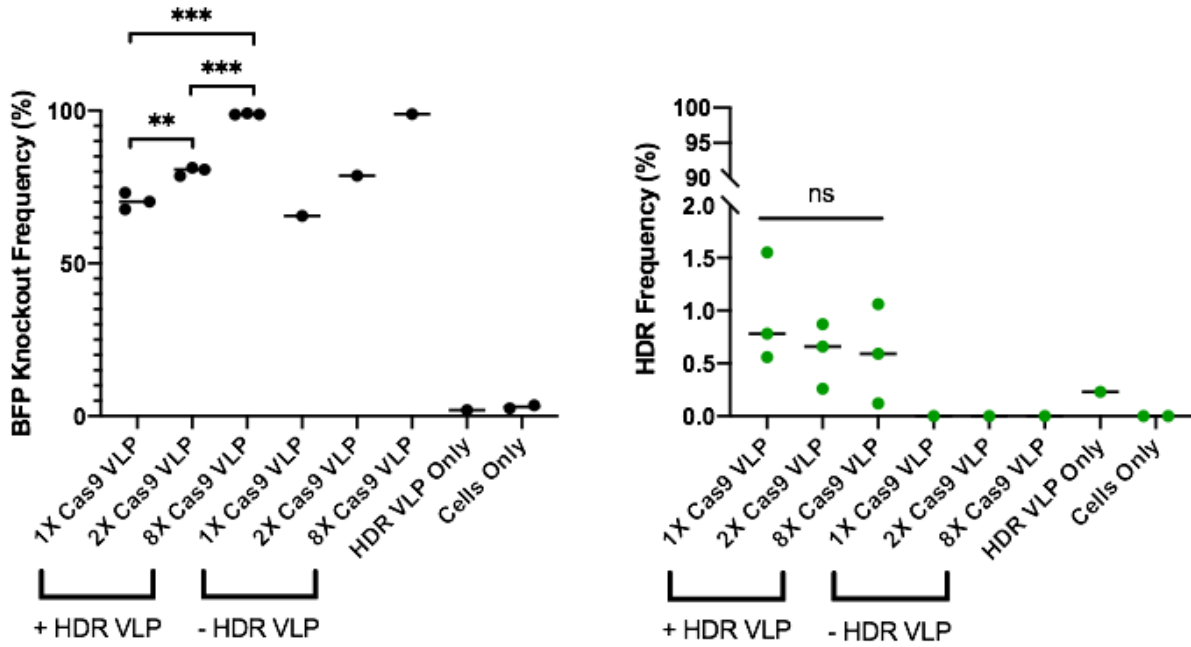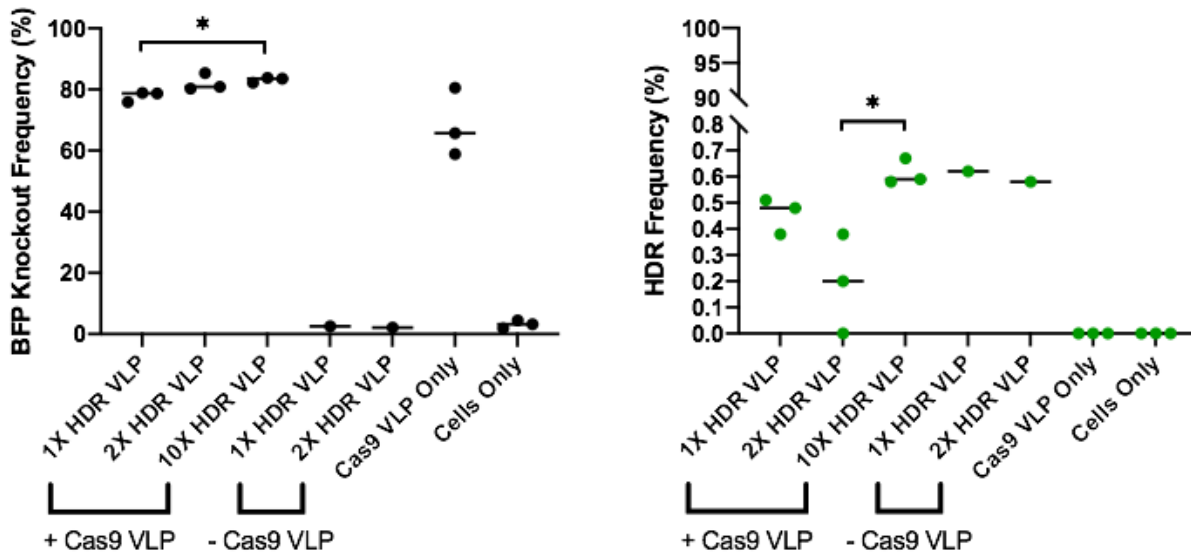
Figure 6a.

b.
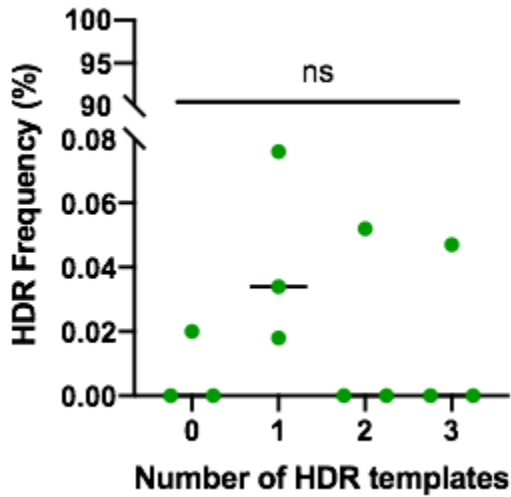
Figure 6c.

Figure 6e.

Figure 6. The dual-VLP system induced Cas9-mediated HDR. **a**, BFP 293T cells were co-treated with two VLPs. The "Cas9 VLP" packaged the anti-*BFP* Cas9 RNPs while the "HDR VLP" delivered the lentiviral genome encoding the HDR repair template(s). **b**, BFP knockout and HDR frequencies in cells that were treated initially with 1X concentrated HDR VLPs and were then treated with 1X concentrated Cas9 VLPs a day later (n=3 for treatments; n=1 for controls). Data were collected 7 days post-transduction. **c**, BFP knockout and HDR frequencies in BFP 293 T cells that were treated simultaneously with 1X concentrated HDR VLPs and Cas9 VLPs at increasing concentrations (n=3 for treatments; n=2 for cells only control; n=1 for HDR VLP only and Cas9 VLP only controls). Data were collected 7 days post-transduction. **d**, BFP knockout and HDR frequencies in BFP 293 T cells that were treated simultaneously with 1X concentrated Cas9 VLPs and HDR VLPs at increasing concentrations (n=3 for treatments, Cas9 VLP only, and cells only; n=1 for HDR VLP only controls). Data were collected 7 days post-transduction. For (**b-d**), the HDR VLPs carried one copy of the repair template on the transfer genome. **e**, HDR frequencies in cells that were treated with Cas9 VLPs and HDR VLPs encoding 0 to 3 copies of the HDR template (n=3). Cas9 and HDR VLPs were both 2X concentrated. Data were collected 3 days post-transduction. The median for each treatment is shown as a horizontal bar. Each data point represents one population of treated cells, and in (**b-d**), each cell population is represented twice across the two graphs, once according to the percentage of BFP- cells in the population and once according to the percentage of HDR+ cells in the population. An ANOVA and Tukey's post hoc test were used for all statistical analyses (*P<0.05, **P<0.01, ***P<0.001; ns, not significant).